Prevention of Lean Flame Blowout using a Real-Time Chemical Reactor Network

Saurabh Gupta

A thesis
submitted in partial fulfillment of the
requirements for the degree of

Master of Science in Mechanical Engineering

University of Washington
2018

Committee
Igor Novosselov
Philip Malte
John Kramlich

Program Authorized to Offer Degree:
Department of Mechanical Engineering

University of Washington

Abstract

Prevention of Lean Flame Blowout using a Real-Time Chemical Reactor Network

Saurabh Gupta

Chair of the Supervisory Committee
Dr. Igor V. Novosselov
Department of Mechanical Engineering

Gas turbine engines are usually operated at lean equivalence ratios (typically about 0.45 to 0.60) in order to achieve better fuel efficiency and to limit NOx emissions, but this increases the risk of the occurrence of a lean flame blowout (LBO). LBO can cause critical safety concerns for aero-based gas turbine engines while for land-based gas turbines, predominantly used for power generation, such a phenomenon can result in expensive and time-consuming shutdown and restart procedures. Previous research shows that the proximity to such a blowout condition in a premixed combustor can be predicted using the combustion species data obtained from a real-time Chemical Reactor Network (RT-CRN) model. The main advantage of this novel technique is that unlike most of other LBO prediction methods which require significant hardware modifications for monitoring of optical or acoustic parameters of the system, this technique uses computational results based on the combustor temperature only and not requiring any additional combustor modifications.

This thesis develops a generic approach for a controlling LBO in a combustor based on the RT-CRN prediction methodology. All calculations shown here are based on experiments conducted in a laboratory single-jet stirred reactor (JSR) operated at atmospheric pressure on methane fuel, which is designed to represent the flame zone of practical combustors. This

approach, however, can be easily extrapolated to other systems, contingent on the availability of a working CRN model for the system and a detailed analysis of the OH-radical behavior across the elements thereof. The algorithm utilizes a 3-element CRN design for the JSR, developed and validated by Kaluri [1]. This design employs a series of three Perfectly Stirred Reactors (PSRs) to model the flame, post-flame and recirculation regions of the JSR respectively. The full GRI 3.0 chemical kinetic mechanism is used for calculating the concentrations of the combustion species in the CRN code.

The proposed methodology is validated by experiments conducted on the JSR apparatus. For all these validation experiments, the air flow in varied as the independent variable and the fuel flow control signal is actuated based on the output of the control algorithm. Two independent sets of experiments are conducted by increasing the system airflow (i) as a step function and (ii) as a monotonically increasing function. The results are examined to confirm the functionality of the devised LBO prevention scheme in terms of its ability to identify and prevent an incipient blowout and to stabilize the system once such an event has been averted.

Table of Contents

LIST OF FIGURES

LIST OF TABLES

ACKNOWLEDGEMENTS

I would like to express my heartfelt gratitude towards Prof. Igor Novosselov for giving me the opportunity to work on this project and for his unique insights and persistent mentoring, over the course of this research. I would also, like to thank him for providing me with the financial support which I needed to accomplish this feat.

I would like to thank Prof. Philip Malte for sharing his rich experimental experience and his in-depth knowledge of the basic subject matter. Special thanks to him for advising me through the calibration process for the experiments without which this work would not have been possible.

I am also, grateful to Prof. John Kramlich for getting me equipped with the fundamentals needed for this research through the various courses he taught me over my time here and for his willingness and enthusiasm to help me out with any doubts or problems as and when required.

My sincere thanks to all my colleagues in the NRG lab for their help and cooperation through the different stages of this research. Special thanks to Abhishek Kaluri for familiarizing me with the experimental setup and basic concepts of this research as a whole and to Anmol Purohit for patiently helping me out during the experiments.

Lastly, I would like to thanks my family – my parents and my sister, and all my friends for inspiring me to pursue this dream of mine and for their unwavering love and support throughout this journey.

Chapter 1. Introduction

1.1 Motivation

Fossil fuels have served as the principal energy resource for humans for decades from the early days of the Industrial Revolution. Rapid technological progress coupled with the swift rise in population has escalated the demand for power. Cleaner renewable energy sources like hydropower, wind and solar energy have gained momentum over the last few decades but are still incapable of fully supporting the rising energy demand. Consequently, fossil fuels are predicted to continue playing a major role in the power generation scene in the foreseeable future. Natural gas is a cleaner fossil fuel option compared to coal owing to lower SO_2 and particulate matter (PM) emissions and reduced CO_2 output per unit of power [2] because of a higher hydrogen to carbon ratio [3] and higher efficiency of power conversion technologies i.e. ~60% for combined cycle power plants to 30-35% for coal-fired plants. However, NOx emissions continue to remain a major concern for natural gas based combustion systems.

NO_x species are known for their various harmful effect on flora and fauna as well as human health. In the presence of sunlight, NO_x combines with volatile organic compounds in the atmosphere to form aerosols and ground-level ozone, also known as photochemical smog. This has adverse effects on vegetation as on the respiratory systems of humans. NOx also combines with water vapor in the air to form acid rain, which is a major cause of soil degradation along with other damaging influences on animals and human life.

The NO_x ($NO+NO_2$) production during a combustion process can broadly be classified as (i) Thermal NOx (formed from combination of atmospheric N_2 and O_2 at elevated temperatures), (ii) Fuel NO_x (formed from reaction of organically bound nitrogen from the fuel with O_2) and (iii) Prompt NO_x (formed by the reaction of hydrocarbon radicals with atmospheric nitrogen to produce HCN and subsequent NOx formation via a complex series of gas phase reactions). Rutar and Malte [4] have further explained this NOx formation process via four interdependent reaction pathways, namely Zeldovich, Nitrous oxide, Fenimore prompt and NNH pathways. All these processes estimate a close dependence of NO_x formation rates on the fuel-air ratio and the flame temperature. Therefore, an effective method to reduce NO_x emissions is Lean Premixed combustion (LPC), which ensures uniformly low fuel-air ratios over the combustion chamber along with low flame temperatures.

Design and operational challenge for LPC process can be Lean Blowout (LBO) of the flame. Land-based gas turbine combustors, used in power generation systems, are often pushed to operate under conditions close to the lean blowout regime during low power operations or when sudden load drops are encountered. The primary reason for this being that the air flow control is sluggish as compared to the fuel flow control, mainly due to the inertia of the compressor, and therefore, during a dip in power demand the reduction in fuel flow occurs faster than the airflow, which destabilizes the fuel-air ratio [5]. A restart procedure resulting from such a blowout event can have huge financial and time-related implications. Similar blowout conditions may also be encountered by aero-engines during throttling operations. During the descent, an aircraft encounters an increase in air density with lowering altitude, which can also destabilize the equivalence ratio. This is a critical safety concern, to counteract which aero-engines are operated with a wide safety margin, resulting in increased time for descent and wastage of expensive aviation fuel [6].

1.2 Lean Flame Blowout – Definition and Identification

A lean flame blowout can be defined as the phenomenon of extinction of a flame due reduction of equivalence ratio beyond a minimum threshold limit. In the words of Heyne et al. [7], 'Lean Blowout' (LBO) is typically defined as the lower limit equivalence ratio that geometry at a given condition can sustain a flame." Longwell et al. [8] related the stability of flame directly to the residence time of the reactants, which in turn is a function of their mass flow rates and the reactor geometry. The LBO process depends both on the rate of chemistry and the gas residence time in the flame stabilization region. Early research was primarily based on correlating the blowout based on experimental results to Damkohler number (Da). The Damkohler number is defined as the ratio of mixing time to the chemical time (τ_{mix}/τ_{chem}). Longwell et al. [8] proposed that blowout occurs when the rate of entrainment of reactants into the recirculation zone cannot be balanced by the rate of burning of those gases. Recently, the effect of local Da non-uniformity in the reactor on LBO has been investigated [9] suggesting that Da gradients in the reactor can lead to local flame extinction, on-set of flow instabilities resulting in LBO. Williams et al. [10] defined flame stability in terms of the balance between flame propagation speed and the flow velocity of the reactants. The same concepts were also employed by Kedia and Ghoniem [11, 12] to describe flame stability for different flow regimes. Chaudhuri et al. [13] explained lean flame blowout as a consequence of high local strain at the flame front and shear layer caused by a drop in flame speed

at lower equivalence ratios. On the other hand, Chao et al. [14] and Stöhr et al. [15] cited the development of high strain rates at the base of a flame as a dominant factor for extinction. Yamaguchi et al. [16] described the structure of a flame in terms of small-scale eddy-flames and lump flames, claiming that global blowout is triggered by local extinction of these eddy-flames.

Owing to the expensive and potentially dangerous implications, blowout prediction has always been a field of interest for researchers. Early research in the identification and prevention of LBO in gas turbines combustors by Snyder et al. [17] indicated the appearance of pressure fluctuations in the combustion chamber. Domen et al. [18] also showed that the increased randomization in the pressure fluctuations, based on a multiscale entropy and nonlinear forecasting method, could be used to predict and control an incipient LBO. Nair and Lieuwen [19] demonstrated that flame blowout is characterized by an increase in low-frequency acoustic emissions. Li et al. [20] observed an exponential increase in low-frequency temperature fluctuations near LBO. A control mechanism was also designed for an experimental swirl-stabilized combustor, involving modulation of the fuel flow when proximity to an LBO was detected, based on the FFT analysis of the feedback signals from a tunable diode laser temperature sensor.

Several researchers have designed LBO prediction techniques based on optical measurements from the combustor, which are mainly used to estimate concentrations of targeted free radicals. Mukhopadhyay et al. [21] utilized symbolic analysis of time series data of CH* chemiluminescence for LBO prediction. Yi and Gutmark [22] observed intensified, low-frequency oscillations in pressure and OH* (hydroxyl free radical) chemiluminescence near LBO conditions and recommended prediction of an incipient blowout on the basis of statistical analyses of such precursor events. Muruganandam et al. [23] also utilized OH chemiluminescence and a threshold-based identification strategy to detect LBO precursor events, and an increased frequency of such events was observed when LBO was approached. These authors also proposed a prevention strategy for an incipient blowout by redistribution of fuel between the main and a pilot flame [24]. Zubrilin et al. [25] also, demonstrated the benefits of using a pilot flame approach in terms of lowering the LBO limit for a methane (CH_4) flame, using steady and transient 3D simulations. OH, radical concentrations have been utilized for LBO prediction by many other researchers, including Vijlee [26], Kaluri [1], Griebel et al. [27], Schefer [28]. LBO control was implemented

on methane flames hydrogen (H_2) pilot flame and hydrogen-blending with methane by Griebel and Schefer respectively.

In a nutshell, it can be said that lean flame blowout has been studied extensively over the course of the past seven decades and multiple methods for LBO prediction and prevention have already been suggested and successfully demonstrated on experimental combustors.

1.3 Model-based Combustion Control

Combustion control techniques can be broadly classified into two categories – passive combustion control and active combustion control. Passive control methods aim to reduce the susceptibility of the combustion process to unstable conditions through hardware changes like fuel flow redistribution and modifications to combustor geometry. However, the shortcoming to these approaches is that they usually work only over a limited range of operating conditions and are expensive to implement. Active control techniques generate output control signals based on real-time feedback from the system; therefore, they are more adaptive and are capable of stabilizing the flame over a much wider range of conditions. Docquier and Candel [29] suggest that combustor controller operation can be classified into Operating Point Control (OPC) and Active Combustion Control (ACC), where ACC can be further categorized into Active Combustion Enhancement (ACE) and Active Instability Control (AIC). In an OPC approach, the system tries to maintain a certain flame parameter within an operating limit while in ACC, the control objective would be to limit combustion instabilities or to improve the combustion characteristics.

Model-based controllers usually rely on a transfer function for their control of the system. The transfer function can be derived mathematically or empirically; it can be based on an open-loop control or a closed loop control philosophy. In relation to combustion systems, model-based controllers have been extensively used by researchers to control thermos-acoustic instabilities. Morgans and Dowling [30] used the concept of an Open-loop Transfer Function (OLTF) to control thermo-acoustic instabilities firstly, in a laboratory-based Rijke tube experiment and later, in an atmospheric pressure combustion rig. Campos-Delgado et al. [31] tested experimental combustion models based on the concepts of LQG, LQG/LTR and H_∞ loop-shaping for controlling thermo-acoustic instabilities in a swirl-stabilized spray combustor. Hathout et al. [32] demonstrated control of thermo-acoustic instabilities in a combustor based on optimization of a quadratic cost function of the pressure response for a physical model of the combustor. Chu et al. [33] optimized the

performance of a simulated coal-fired boiler using an Artificial Neural Network (ANN) model. Havlena and Findejs [34] used a Model Predictive Control (MPC) method to control the superheated steam pressure for a boiler while maintaining the air-fuel ratio to obtain the desired emission characteristics. Some researchers have also attempted to apply model-based control techniques for prediction of LBO. Hu [35] developed a hybrid flame-volume model for LBO prediction based on the original flame volume concept, proposed by Lefebvre [36] combined with numerical simulations.

In the present work, model-based control approach is investigated for prediction and avoidance of LBO in the jet-stirred reactor (JSR) operating on methane.

Chapter 2. Research Goals and Methodology

2.1 Objectives

The LBO detection techniques listed in Section **Error! Reference source not found.** are based on acoustic or optical methods to identify combustion instabilities or to estimate concentrations of critical combustion radicals. Moreover, combustion control is achieved by the addition of a secondary fuel or by the redistribution of the primary fuel inlet into the combustion chamber. Such methods require bulky and expensive hardware modifications to the combustion chamber. The present work is aimed at achieving similar results, in terms of controlling an incipient LBO, albeit without the requirement of such modifications.

The primary goal of the research is to devise a low-cost method of preventing an incipient lean blowout in a combustor nut without the requirement of any significant hardware additions.

2.2 Technical background and Approach

2.2.1 Jet-stirred Reactors

The jet-stirred reactor is a type of continuously stirred-tank reactor. The presence of a reasonably large recirculation zone ensures the efficient mixing of the gas phase, which provides approximately identical and homogeneous compositions of the outlet gas and of the gas inside the reactor. When operated at steady state and at constant residence time, temperature and pressure, this type of reactor can be modeled by a very simple system of mass balances.

Apart from the computational convenience, it has also been observed from previous work that the combustion properties for JSRs are similar to those in real-life gas turbine engines. Both have two distinct flow features - a jet (i.e. shear layer) and a recirculation zone. Therefore, any results obtained on a JSR setup can be easily extrapolated to these systems. This has made them a popular option for experimental combustors intended to study oxidation and pyrolysis of hydrocarbon fuels. Jet stirred reactors have been extensively used for studying emission characteristics for lean premixed combustion, e.g., Steele et al. [37], Malte and Pratt [38], Rutar and Malte [4] and Moreac [39] among many others.

2.2.2 Chemical Reactor Network Modeling

Chemical reaction network (CRN) theory is a field of applied mathematics, which uses an idealized representation of real-world chemical systems. A CRN model for combustion analysis consists of a single or a series of reactors, which as a system, is capable of approximating the reaction rates and consequently, concentrations of the chemical species (including reactants, products, and intermediate combustion radicals) in order to give an estimate for various physical and thermodynamic properties. Bragg [40] pioneered the concept of numerical modeling of a gas turbine combustor; he employed a Perfectly Stirred Reactor (PSR) to represent the high-intensity primary zone, followed by a Plugged Flow Reactor (PFR) to represent the secondary burnout zone. Swithenbank et al. [41] modeled a gas turbine combustor as a series of interconnected partially stirred reactors based on concepts of turbulent mixing and energy balancing. Based on these concepts, CRN models have been extensively used for analysis of emissions in laboratory-scale combustors, such as in the works of Rutar and Malte [4], Feitelberg et al. [42], Fackler et al. [43], Schlegel et al. [44] and Sturgess and Shouse [45]. This has paved the way for the development of more precise but complex CRN models with ten or more reactor elements, based on the results of CFD simulations of flow field and reaction space in the combustor. Examples of such models have been used by Rubin and Pratt [46], Novosselov [3], Novosselov and Malte [47], Fichet et al. [48] and Lyra and Cant [49] for predicting emissions for industrial gas turbine combustors. The CRN modeling approach has also been used to study LBO by Sigfrid et al. [50] for a Rich-Pilot-Lean (RPL) combustor, Sturgess [51] for aerodynamic gas turbine combustors and Karalus [52] for a JSR. CRN concepts have also been utilized for the study of solid fuel combustion, such as in the works of Robertus, Nielson [53], Benedetto et al. [54], Faravelli et al. [55], Falcitelli et al. [56] and Ranzi et al. [57], to name a few.

Several authors have investigated the numerical implementation of CRN modeling. Related to this work, the in-house CRN code was originally developed by Pratt and co-workers who also applied the software to model high-intensity combustors, e.g., [58-61]. The PSR reactor concept is implemented by balancing the Arrhenius source terms of net production of each species by convective removal of that species from the PSR control volume. The PFR concept is modeled by a series of PSRs. One of the major benefits of the current code is in the implementation of the fast convergence algorithm, which enables near real-time chemical kinetic calculations in complex CRN arrangements [62-65].

The CRN configuration in this work uses GRI 3.0, an optimized chemical kinetic mechanism to model natural gas combustion [37]. It contains 325 reaction steps and 52 species. The GRI 3.0 mechanism has been validated using experimental data for methane, ethane, hydrogen and carbon monoxide. For example, Hu et al. found good agreement between the laminar burning velocities calculated experimentally and computationally using the GRI 3.0 mechanism for the methane-hydrogen-air flame [38]. Flame speed validation [66-69] and ignition delay comparison with experimental data [70], [71] have been reported for GRI 3.0.

2.2.3 Methodology

The JSR CRN for this work is based on networked developed by Kaluri [1]. The model consists of three elements (details explained in Chapter 4). A comparison of the concentration and the trends of OH-radical in the different elements have also been demonstrated as an effective predictor of LBO event. The present work aims at utilizing this concept to demonstrate a control mechanism capable of preventing an incipient LBO event in real-time, based on predictions of a chemical kinetic model. Figure 2.1 shows the schematic diagram of the approach.

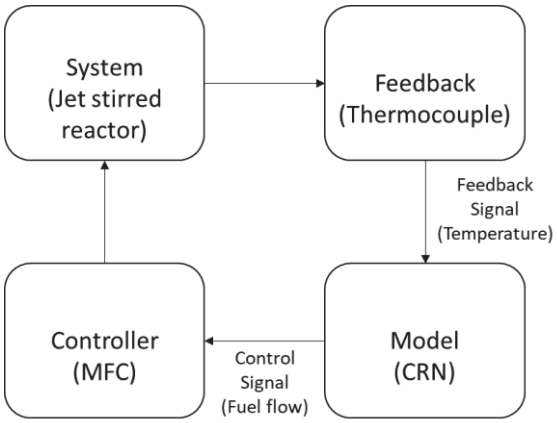

Figure 2.1: Schematic for Research Approach

The following strategy shall be employed to accomplish the desired objective:-

1. Design a control algorithm capable of adjusting the equivalence ratio to prevent an LBO event, based on the computed OH-radical concentrations in the CRN elements, based on the CRN model developed by Kaluri [1].

2. Develop real-time monitoring strategies for input to the algorithm and algorithm output for use in the automated closed-loop control.
3. Demonstrate the use of the closed-loop control for methane combustion in the laboratory JSR setup.

Chapter 3. Experimental Setup

The experimental setup consists of a high intensity, back mixed, single-jet stirred reactor with methane as fuel. The JSR is considered to mimic the primary zone of a gas turbine combustor under laboratory conditions. All user functions for monitoring and control are implemented using LabVIEW interface. The total volume of the JSR used in this study is 15.8 cc. The JSR has two main zones: the jet zone and the recirculation zone. The JSR setup comprises a stainless steel fuel-air premixer, Inconel nozzle block, and a ceramic JSR reactor as shown in Figure 3.1. A premixed fuel-air mixture enters the reactor through a 2 mm choked nozzle. The air and fuel flow into the JSR are metered through Sierra instruments mass-flow controllers (MFC) that are controlled via National Instruments module (MyRio). This circuit is also utilized for monitoring of the air and fuel flows via feedback signal sent back to the LabVIEW interface. The air is supplied from the filtered shop air inlet duct and regulated at 50 psig at the inlet of the MFC. The fuel (CH_4) is supplied from a high-pressure cylinder, again regulated to a pressure of 50 psig upstream of the MFC.

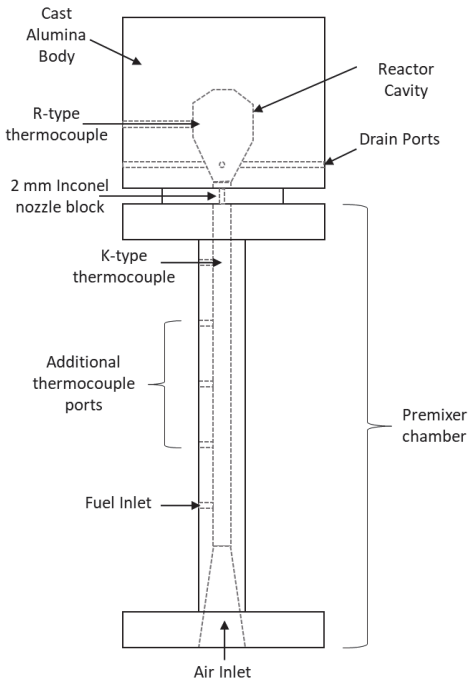

Figure 3.1: Experimental JSR module

The temperature and gas species measurements are conducted at 2/3rd of the JSR height and 3/4th of the width, as depicted in Figure 3.1. An R-type thermocouple (TC) coated with alumina to prevent catalytic temperature gain measures the temperature inside the JSR. K-type thermocouples monitor the temperature of reactants in the premixer. The thermocouple data are relayed to National Instruments LabVIEW software using thermocouple data acquisition (TC DAQ, Omega Systems). For the steady-state experiments in the JSR, the temperature correction due to radiative heat loss to the reactor walls is estimated based on [72] to vary from 21 to 43 degrees K over the range of combustion conditions studied. However, in the transient (i.e., blowout) experiments, the uncertainty in the temperature correction increases due to cooling in the reactor wall, which has large thermal inertia. For consistency, in this work, all temperature data in steady-state and transient experiments, are reported as measured without TC heat loss correction.

The LabVIEW environment provides an integrated platform for monitoring and control of all parameters. In addition to providing the user interface for the experiments, LabVIEW has been used to integrate the real-time CRN program with the experimental input/output signals, as shown in Figure 3.2, in order to achieve the intended control action.

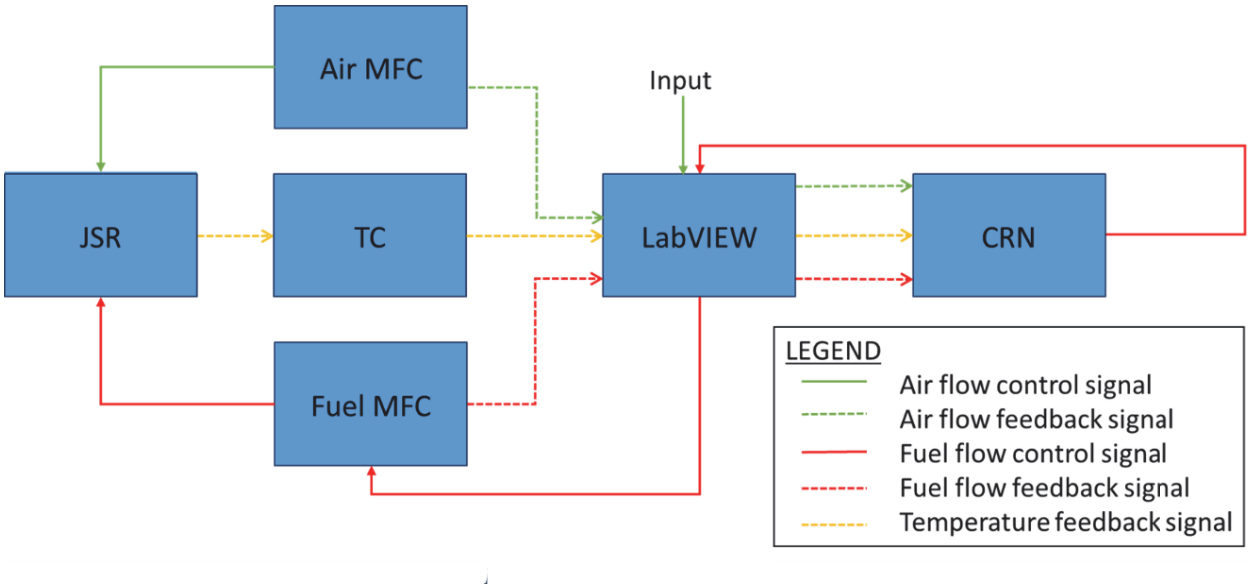

Figure 3.2: Block diagram for the signal flow

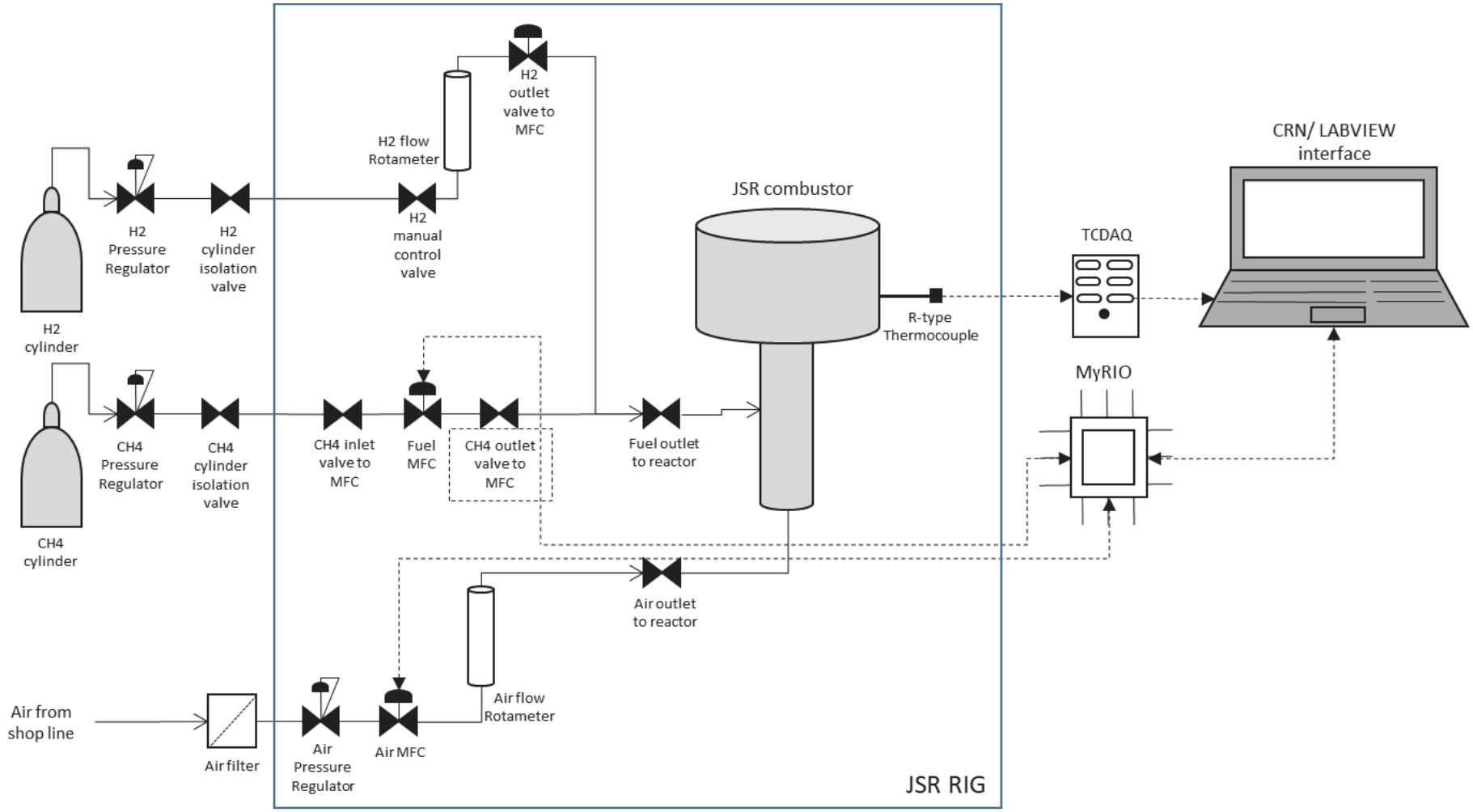

Figure 3.3: Flow scheme for Experimental JSR

Chapter 4. Computational Model

The CRN for prediction of LBO in the JSR has been reported in [1]. This configuration was originally developed based on the previous work [27, 30, 49]. The reactor is modeled as a 3-element CRN, consisting of three perfectly stirred reactors. The jet-flame region is modeled as an adiabatic perfectly stirred reactor (PSR1) with relatively small volume. The recirculation zone can also be modeled as a stirred reactor as the lower mixing rates are accompanied by lower reaction rates. But this zone encounters a high heat transfer from the jet of reactants as well as the reactor walls and is, therefore, modeled as a constant temperature element (PST3) with temperature input equal to the temperature reading taken from the R-type thermocouple. This covers the maximum volume of the reactor. The products from the flame region impinge on the top wall before transitioning into the recirculation zone. In this region, the gases experience a cooling effect due to the impingement effect and proximity to the wall. Therefore, this transition region is modeled as a non-adiabatic PSR, i.e. a post-flame zone (PSR2).

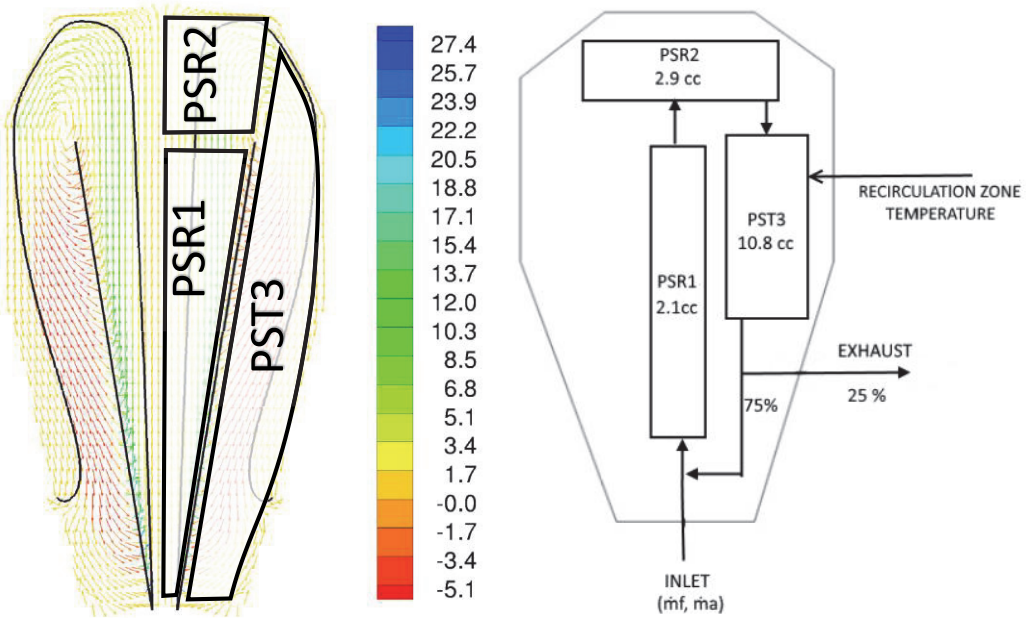

Figure 4.1: (Left) CFD solution for JSR [64]; (Right) CRN Configuration [1]

The exact volumes of the individual elements are decided on the basis of the CFD solution of Karalus [64] followed by finer tuning performed by Kaluri [1] based on the LBO experiments.

Entrainment of 75% of the combustion gases by the jet from the recirculation is considered. This configuration is based on the reactor behavior under stable combustion (Temperature > 1700K), although the flame location may shift during the lower equivalence ratio operations.

For experiments designed for tuning of the CRN, a gas sample was extracted from the recirculation region of the JSR, corresponding to PST3 of the CRN model, and passed through a Horiba VA 3000 gas analyzer unit to obtain the concentrations of CO, CO_2, and O_2 respectively. The experimental concentrations were then compared to the predictions from the CRN, and the volumes of the individual elements were readjusted, keeping the total volume constantly equal to the physical volume of the JSR until a satisfactory agreement was achieved between the CRN computed values and the experimental data. This process was repeated at different steady-state conditions, i.e. flow conditions for fuel and air at which a sustained flame could be obtained. The individual CRN reactor volume was adjusted to achieve the best agreement over a range of the steady state conditions for CO_2, CO, and O_2 data. These data can be found in [1].

Chapter 5. Control Module

5.1 Model-based control approach

The OH radical is an intermediate radical produced during hydrocarbon combustion. Kaluri [1] reported OH radicals concentration the JSR CRN elements for various Φ for steady and transient operation during reactor cooling down. Figure 5.1 plots the data obtained from one of these experiments on the JSR. For each experimental case, the JSR is set at an initial equivalence ratio of Φ = 0.8 and warmed up to a steady-state temperature of $T_{initial}$ = 1730-1780 K (uncorrected for thermocouple heat loss). The range in the initial temperature is caused by day-to-day variations in the ambient lab temperature, small variations in the initial Φ, small differences in placement of the thermocouple in the JSR, and changes in the condition of the thermocouple coating. Following the warm-up period of the JSR, a step change is executed in the fuel flow rate, thereby reducing the Φ to a level that cannot sustain stable combustion in the reactor. Once the Φ is reduced, the temperature inside the reactor drops. During this period, the CRN operating in real-time prediction mode (RT-CRN) uses the reactor temperature measurement as the PST3 input; and the CRN solution is updated in real time.

The OH trends and ratios between zones were used as criteria for predicting the proximity to combustor blowout. Three distinct events are observed in the RT-CRN modeling. At steady-state combustion, the OH levels are high, ranging from about 0.45% (by volume) in the near post-flame zone (PRS2) to about 0.3 % in the recirculation zone (PST3). Immediately after reducing the Φ (from 0.80 to 0.62), the OH concentrations in the three zones decreases significantly. *Event 1* corresponds to the concentration of OH in PSR1 falling below the level in PST3. At a later time (i.e., at about 6 s), PSR1 fails to maintain a burning solution. PSR1 blows out. This is *Event 2*. Once PSR1 blows out, the PST3 OH concentration stabilizes, representing the movement of flame downstream. Eventually, the OH concentration in PSR2 falls below the level in PST3. This is *Event 3*. The OH level in PSR2 diminishes further indicating the further movement of flame into recirculation zone.

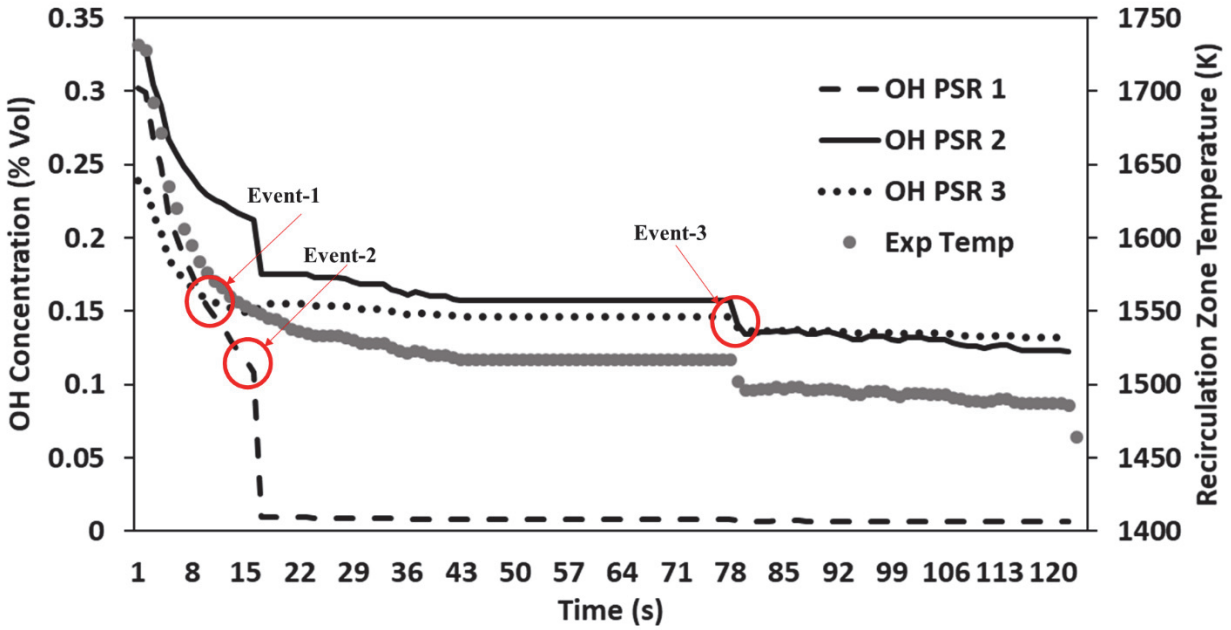

Figure 5.1: Behavior of OH radical concentration at LBO, from [1]

Based on the transient experiments the flame is most stable before Event 1, i.e., flame blowout in the first element. Hence, our control objective in this work to prevent the occurrence of Event 1 by adjusting the fuel flow rate and stabilizing the system if it approaches OH ratio threshold as defined by Event 1. In the experiments described in this work, the combustor can approach *Event 1* by the gradual increase the air flow rate or by sudden increase the air flow rate resulting in the gradual decrease in the reactor wall temperature. Another control objective is to maintain fuel economy in the system while maintaining stable combustion; hence, the amount of fuel added, for LBO prevention, should be minimal.

5.2 Algorithm

As shown in Figure 5.1, the Event 1 can be detected by comparing the OH concentration values in elements PSR1 and PST3. Hence, we define a control parameter:

$$OH\ ratio = \frac{OH\ concentration\ in\ PSR1}{OH\ concentration\ in\ PST3}$$

Since the desired control point requires that

$$OH\ concentration\ in\ PSR1 = OH\ concentration\ in\ PST3$$

i.e.

$$OH\ ratio = 1$$

+ Therefore, the control algorithm shall attempt to maintain this control parameter as:

$$OH\ ratio = 1 \pm 5\%$$

As the OH ratio approaches the threshold for the Event 1, reactor approaches a well-stirred regime with minimum OH concentration gradient between jet and recirculation regions.

During experimental runs, the OH is calculated in RT-CRN, and the OH ratio is reported. No adjustment to fuel flow is made for values of $OH\ ratio \geq 1.2$. Under this condition, the combustion is stable and therefore the control algorithm remains on the stand-by. At all values of OH ratio less than this threshold, the control code will take over the control of the fuel flow MFC and manipulate the fuel flow based on the results from the control algorithm, depicted in Figure 5.2.

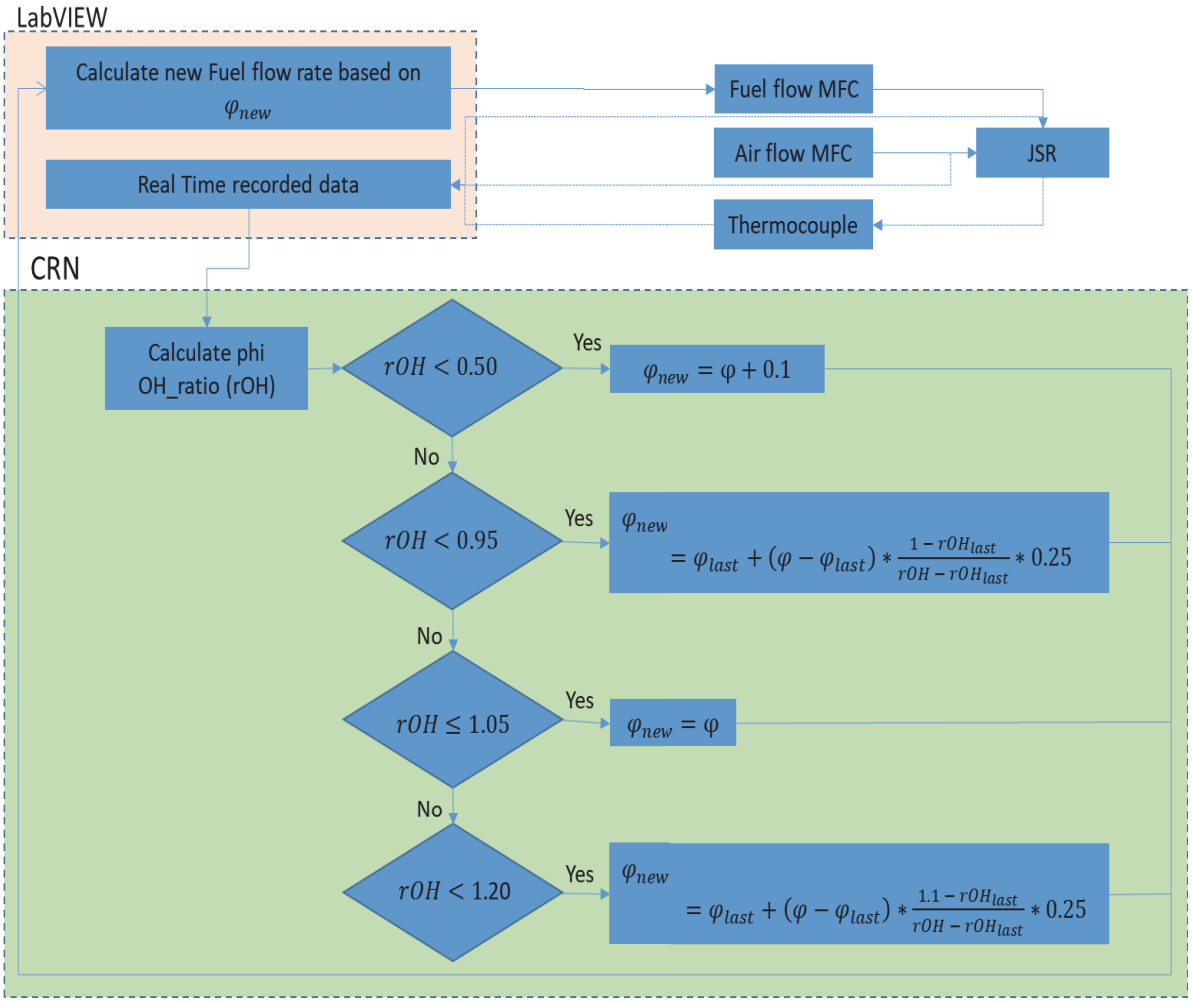

Figure 5.2: Control Algorithm

The present algorithm is based on a proportional control principle. The modified CRN code accepts the mass flow of air and fuel and the JSR temperature as inputs to calculate the existing Φ -value, and based on the formulae calculates a new Φ-value ($\Phi_{new,}$) which should be able to maintain the system about the control point mentioned earlier. This Φ_{new} is fed to the LabVIEW interface that converts it to a fuel flow control signal, which is subsequently relayed to the fuel flow MFC. All constants involved here have been adjusted empirically. In these experiments control module was set maintained the OH ratio in the range of 0.95-1.2 by proportional adjustments of fuel flow rate based on the Φ calculated in the previous iteration. Accept in the conditions when OH ratio <0.5, there Φ was increased by a value of 0.1 to accelerate the system recovery.

Chapter 6. Experimental Validation of Control System

The performance of the developed control algorithm was evaluated using JSR described in chapter 2. For the purpose of the experiments, the air flow was chosen as the independent variable, and fuel flow was used as the model-based actuator. The air flow into the JSR was varied using two different scenarios:

1. Step function
2. Monotonically increasing function

6.1 General Experimental Procedure

In all experiment, the JSR was first ignited, using the procedure detailed in Appendix II. The air flow is set to a value of 0.8 g/s, and equivalence ratio is set to 0.75. The reactor is allowed to stabilize to a steady state temperature, under these conditions. Once the steady state is achieved, the fuel flow control is shifted to "auto" mode, so that the algorithm controls the fuel flow command signal subsequently. The air flow can be set manually. All the parameters listed in Table 6.1 are recorded until the system stabilizes to a relatively steady value of experimental JSR temperature.

Table 6.1: Control Parameters

Set and Measured Parameters	Computed parameters
1. Air flow rate 2. Initial fuel flow rate 3. JSR temperature	1. Temperatures for individual CRN elements 2. Concentration of OH radical for individual CRN elements 3. OH ratio (PSR1/PRS3) 4. Output Φ_{new} from the control algorithm (new fuel flow rate)

6.2 Experiment set 1

The first set of experiments were conducted by increasing the air flow as a step function from a lower to a higher value. Each independent trial was conducted with a different final value of air flow rate, as shown in Table 6.2.

Table 6.2: Cases for Experiment Set# 1, the case in bold is taken as the baseline case.

Case #	Lower Air flow limit (g/s)	Higher Airflow limit (g/s)
1	0.8	1.0
2	0.8	1.1
3	**0.8**	**1.2**
4	0.8	1.3

The behavior of the system was observed to be similar for all the cases. Case 3 is used as the baseline to demonstrate the algorithm performance for step-function air increase. For plotting, the time zero has been set at the change in air flow is initiated. Figure 6.1 shows the basic behavior of the control algorithm. After the change in the airflow, the predicted OH ratio dips steeply, and the system approaches an LBO condition. However, such a blowout event is averted as the algorithm takes corrective action by increasing the equivalence ratio (fuel flow rate). The system undergoes a few fluctuations in OH ratio and the consequent modulations in equivalence ratio before a moderately steady condition is achieved.

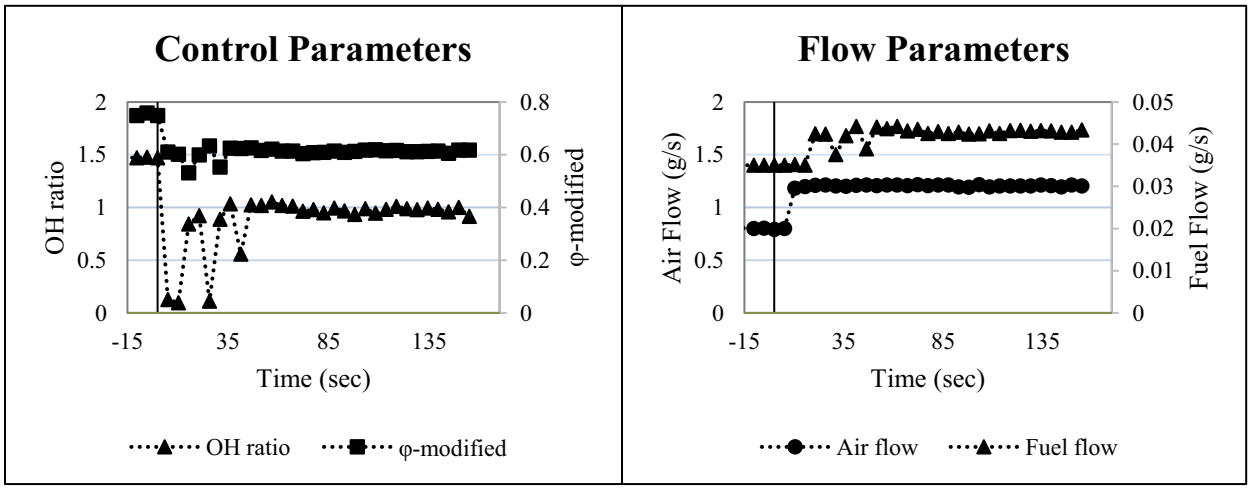

Figure 6.1: (Left) Time variation of control parameters for Experiment set# 1, Case# 3; (Right) Time variation of flow data for Experiment set# 1, Case# 3

Figure 6.2 shows the respective temperatures and OH radical concentrations computed for each element of the CRN. The behavior of both curves for each element is similar since the OH concentrations are primarily a function of the temperature

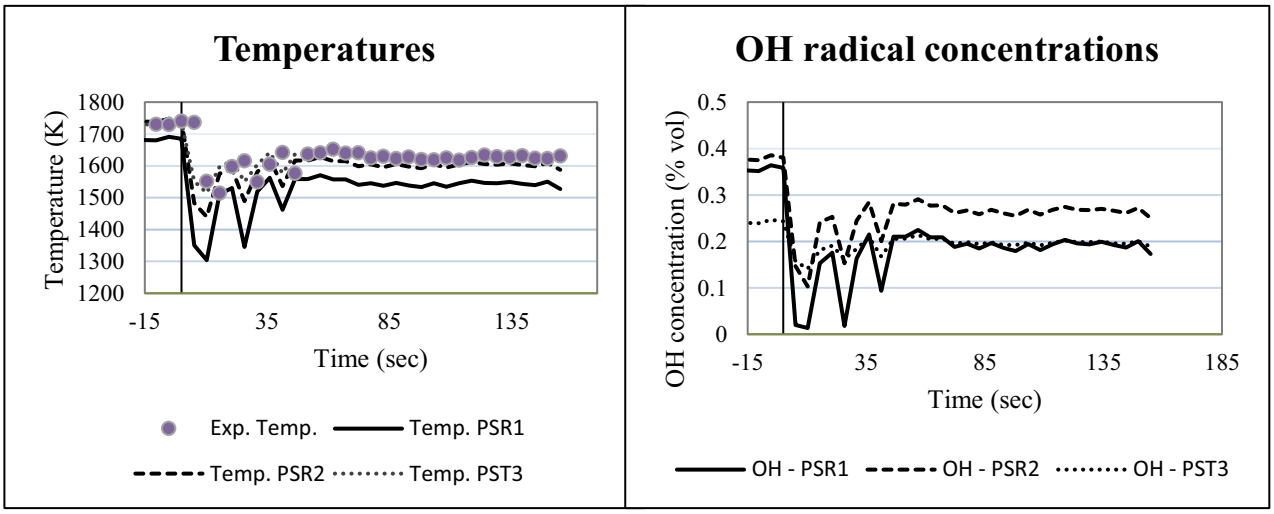

Figure 6.2: (Left) Time variation of Temperatures (measured and computed) for Experiment set# 1, Case# 3; (Right) Time variation of computed OH concentrations for Experiment set# 1, Case# 3

Table 6.3 compares the control performance for the different cases in experiment set# 1 with respect to some critical indicators. The initial response time is the time period between the initial increase in air flow and the first alteration observed in the fuel flow. Since this experiment involves an instantaneous jump in the air flow, i.e. a step increase, the initial response time is observed to be approximately the same for all cases. The response time includes several hardware time delays, computational delay related to CRN convergence, and the time of the thermochemical response of the combustion system. Among the hardware delays are thermocouple response delay in measuring the reactor temperature, mass flow controller delays in regulating the flow rate, these are in the order of few seconds. The time required to converge the CRN solution was around 5 seconds. The response time related to thermochemical properties of the reacting system is harder to estimate since for each condition the time to reach the onset of the algorithm response is different due to variation in the real-time species composition, gas and wall temperatures. However, these delays do not add to each other serially, but rather are a convolution of several processes that may be taking place at the same time.

The stable condition is identified when a stable value of $OH\ ratio = 1.00 \pm 0.05$ $(0.95 - 1.05)$ is reached. At this condition, the experimental parameters such as equivalence ratio and temperature do change significantly. The mean for each of these parameters under the stable conditions are shown in Table 6.3. The mean values for the experimental equivalence ratio for the stabilized condition of the system for all cases is observed to be similar; however, the difference in air flow rates results in some differences in the mean stable temperature values. The values reported here are not the steady state conditions that would be achieved after the rector reaches the new steady state (15-20 min) but the conditions under which the algorithm is able to stabilize the reactor. After the stabilization the JSR walls are still cooling down; the steady state condition for the set control point would have higher Φ, as more fuel is needed when the reactor wall reach lower steady state temperature.

Table 6.3: Control parameters for Experiments in set# 1, step function air increase

	Initial response time (sec)	Stabilization time (sec)	Mean OH ratio under stable condition	Mean Φ under stable condition	Mean Experimental Temp. under stable condition (K)
Case 1	15	57	0.952	0.62	1575
Case 2	16	109	0.966	0.61	1602
Case 3	15	31	0.993	0.61	1630
Case 4	15	31	0.965	0.62	1641

6.3 Experiment set 2

The second set of experiments was conducted by increasing the air flow as a monotonically increasing function, i.e., the air flow was ramped-up from a lower value to a higher value over a specific period of time. Each independent trial was conducted with a different ramp time, as shown in

Table 6.4. Again, a characteristic behavior was observed for all the listed cases. This behavior shall be discussed by considering the results from trial # 4 as a sample case.

Table 6.4: Cases for Experiment Set# 2

Case #	Lower Air flow limit (g/s)	Higher Air flow limit (g/s)	Ramp Time (sec)
1	0.8	1.2	360
2	0.8	1.2	240
3	**0.8**	**1.2**	**180**
4	0.8	1.2	120
5	0.8	1.2	60
6	0.8	1.2	30

Figure 6.3 depicts behavior similar to that observed for experiment set# 1. The gradual rise in airflow triggers an LBO condition, although somewhat delayed. The control algorithm is again successful in preventing a blowout, and the system is subsequently stabilized.

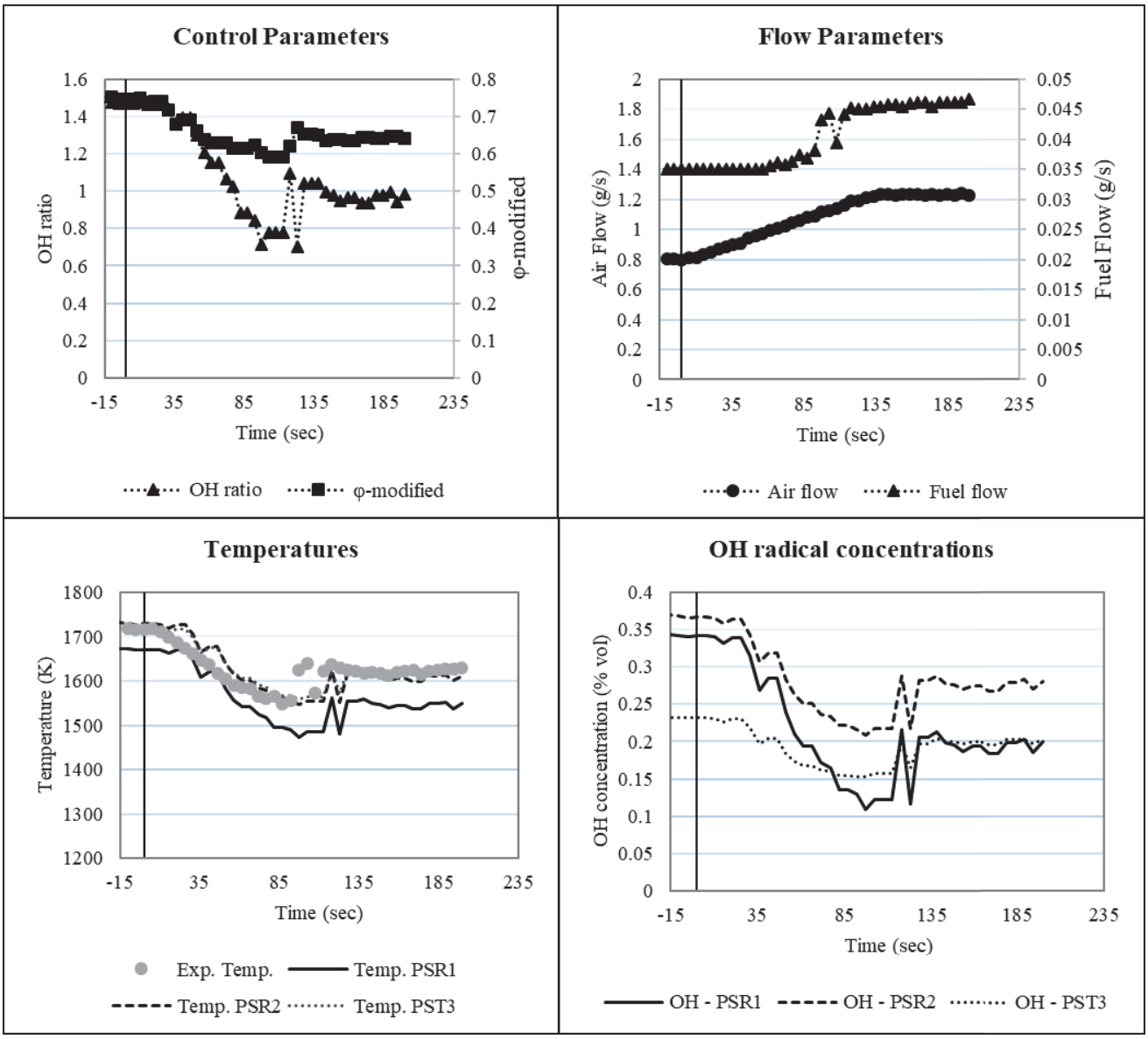

Figure 6.3: Time variation of parameters for Experiment set# 2, Case# 3

Table 6.5 shows the results for 6 cases with varying air flow rate ramp-up times. Since the rate of air flow ramp-up decreases progressively from Case 1 to Case 6, the initial response time follows an increasing trend. This is due to slower reactor response time as the Φ changes gradually as well as reactor wall cooling is slower for a lower rate of change Φ. The algorithm response is also slower than in the experiments with step function change. The stabilization times increase due to continuingly changing air flow. Criteria for stability being the same as that in Experiment set 1 case 3; however, the resulting is higher as the reactor walls able to cool down further than in

the step experiment. The mean value of the OH ratio under the stable condition is found to be within the correct range defined for the algorithm.

Table 6.5: Comparison of control parameters for all cases in Experiment set# 2

	Initial response time (sec)	Stabilization time (sec)	Mean OH ratio under stable condition	Mean Φ under stable condition	Mean Experimental Temp. under stable condition (K)
Case 1	26	26	0.985	0.643	1625
Case 2	26	31	0.981	0.642	1622
Case 3	36	56	0.978	0.642	1621
Case 4	51	51	0.977	0.641	1620
Case 5	61	102	0.980	0.643	1620
Case 6	94	427	1.043	0.641	1635

Chapter 7. Conclusions

This research demonstrates a proof-of-concept for a non-invasive methodology of preventing an incipient lean blowout by modifying the equivalence ratio of the system. The identification of the onset of a blowout is primarily based on the computed concentrations of a critical combustion species, i.e., OH radical using a chemical reactor network. A three-element CRN configuration using three perfectly stirred reactor elements, namely PSR1 (for the flame zone), PSR2 (for the post-flame zone) and PST3 (for recirculation zone), originally suggested by Kaluri [1], is utilized for the computations.

The control approach is based on a ratio of the OH radical concentrations of elements PSR 1 (jet region) and PSR3 (recirculation zone). The devised control algorithm is based on a proportional control formula. The performance of the mechanism is evaluated in terms of its ability to prevent an LBO event bringing the system to a stable operating condition. Satisfactory results are obtained under the various experimental condition to confirm the effectiveness of the devised method.

The present work successfully demonstrates a general approach to a low-cost LBO prevention method. Application of this methodology to other system require additional investigation. Firstly, a working CRN model of the system in question needs to be developed using CFD simulations and/or experimental methods. Another important preparatory step would be to analyze the OH behavior across the different elements of the developed model to determine proper control parameter and establish the operating limits to prevent a blowout. The present approach employs a proportional control approach. It is possible that more sophisticated control approaches can be used to obtain better results.

REFERENCES

[1] A. Kaluri, "Real-Time Prediction of Lean Blowout using Chemical Reactor Network," Mechanical Engineering, University of Washington, Seattle, 2017.

[2] K. Hayhoe, H. S. Kheshgi, A. K. Jain, and D. J. Wuebbles, "Substitution of natural gas for coal: climatic effects of utility sector emissions," *Climatic Change,* vol. 54, no. 1-2, pp. 107-139, 2002.

[3] I. V. Novosselov, "Eight-Step Global Kinetic Mechanism on Methane Oxidation with Nitric Oxide Formation for Lean-Premixed Combustion Turbines," University of Washington, 2002.

[4] T. Rutar and P. C. Malte, "NOx Formation in High-Pressure Jet-Stirred Reactors with Significance to Lean-Premixed Combustion Turbines," *ASME Journal of Engineering for Gas Turbines and Power,* vol. 124, pp. 776-783, 2002.

[5] L. Meegahapola and D. Flynn, "Characterization of gas turbine lean blowout during frequency excursions in power networks," *IEEE Transactions on Power Systems,* vol. 30, no. 4, pp. 1877-1887, 2015.

[6] T. J. Rosfjord and J. M. Cohen, "Evaluation of the transient operation of advanced gas turbine combustors," *Journal of Propulsion and Power,* vol. 11, no. 3, pp. 497-504, 1995.

[7] J. Heyne *et al.*, "Year 2 of the National Jet Fuels Combustion Program: Moving Towards a Streamlined Alternative Jet Fuels Qualification and Certification Process," in *AIAA SciTech Forum*, 2017.

[8] J. P. Longwell, E. E. Frost, and M. A. Weiss, "Flame stability in bluff body recirculation zones," *Industrial & Engineering Chemistry,* vol. 45, no. 8, pp. 1629-1633, 1953.

[9] Y. Guan and I. Novosselov, "Damkohler number analysis in Lean Blowout of Toroidal Jet Stirred reactor," *Journal of Engineering for Gas Turbines and Power,* Technical Brief vol. Accepted, no. GTP-17-1495, March 2018 2018.

[10] G. C. Williams, H. Hottel, and A. C. Scurlock, "Flame stabilization and propagation in high velocity gas streams," in *Symposium on Combustion and Flame, and Explosion Phenomena*, 1948, vol. 3, no. 1, pp. 21-40: Elsevier.

[11] K. S. Kedia and A. F. Ghoniem, "The blow-off mechanism of a bluff-body stabilized laminar premixed flame," *Combustion and Flame,* vol. 162, no. 4, pp. 1304-1315, 2015.

[12] K. S. Kedia and A. F. Ghoniem, "Mechanisms of stabilization and blowoff of a premixed flame downstream of a heat-conducting perforated plate," *Combustion and Flame,* vol. 159, no. 3, pp. 1055-1069, 2012.

[13] S. Chaudhuri, S. Kostka, M. W. Renfro, and B. M. Cetegen, "Blowoff dynamics of bluff body stabilized turbulent premixed flames," *Combustion and flame,* vol. 157, no. 4, pp. 790-802, 2010.

[14] Y.-C. Chao, Y.-L. Chang, C.-Y. Wu, and T.-S. Cheng, "An experimental investigation of the blowout process of a jet flame," *Proceedings of the Combustion Institute,* vol. 28, no. 1, pp. 335-342, 2000.

[15] M. Stöhr, I. Boxx, C. Carter, and W. Meier, "Dynamics of lean blowout of a swirl-stabilized flame in a gas turbine model combustor," *Proceedings of the Combustion Institute,* vol. 33, no. 2, pp. 2953-2960, 2011.

[16] S. Yamaguchi, N. Ohiwa, and T. Hasegawa, "Structure and blow-off mechanism of rod-stabilized premixed flame," *Combustion and Flame,* vol. 62, no. 1, pp. 31-41, 1985.
[17] T. S. Snyder and T. J. Rosfjord, "Active gas turbine combustion control to minimize nitrous oxide emissions," ed: Google Patents, 1998.
[18] S. Domen, H. Gotoda, T. Kuriyama, Y. Okuno, and S. Tachibana, "Detection and prevention of blowout in a lean premixed gas-turbine model combustor using the concept of dynamical system theory," *Proceedings of the Combustion Institute,* vol. 35, no. 3, pp. 3245-3253, 2015.
[19] S. Nair and T. Lieuwen, "Acoustic detection of blowout in premixed flames," *Journal of Propulsion and Power,* vol. 21, no. 1, pp. 32-39, 2005.
[20] H. Li, X. Zhou, J. B. Jeffries, and R. K. Hanson, "Active control of lean blowout in a swirl-stabilized combustor using a tunable diode laser," *Proceedings of the Combustion Institute,* vol. 31, no. 2, pp. 3215-3223, 2007.
[21] A. Mukhopadhyay, R. R. Chaudhari, T. Paul, S. Sen, and A. Ray, "Lean blow-out prediction in gas turbine combustors using symbolic time series analysis," *Journal of Propulsion and Power,* vol. 29, no. 4, pp. 950-960, 2013.
[22] T. Yi and E. J. Gutmark, "Real-time prediction of incipient lean blowout in gas turbine combustors," *AIAA journal,* vol. 45, no. 7, pp. 1734-1739, 2007.
[23] T. Muruganandam, S. Nair, Y. Neumeier, T. Lieuwen, and J. Seitzman, "Optical and acoustic sensing of lean blowout precursors," in *38th AIAA/ASME/SAE/ASEE Joint Propulsion Conference & Exhibit*, 2002, p. 3732.
[24] T. Muruganandam *et al.*, "Active control of lean blowout for turbine engine combustors," *Journal of Propulsion and Power,* vol. 21, no. 5, pp. 807-814, 2005.
[25] I. A. Zubrilin, N. I. Gurakov, and S. G. Matveev, "Lean Blowout Limit Prediction in a Combustor with the Pilot Flame," *Energy Procedia,* vol. 141, pp. 273-281, 2017.
[26] S. Z. Vijlee, I. V. Novosselov, and J. C. Kramlich, "Effects of Composition on the Flame Stabilization of Alternative Aviation Fuels in a Toroidal Well Stirred Reactor," in *ASME Turbo Expo 2015: Turbine Technical Conference and Exposition*, 2015, pp. V003T03A007-V003T03A007: American Society of Mechanical Engineers.
[27] P. Griebel, E. Boschek, and P. Jansohn, "Lean blowout limits and NOx emissions of turbulent, lean premixed, hydrogen-enriched methane/air flames at high pressure," *Journal of engineering for gas turbines and power,* vol. 129, no. 2, pp. 404-410, 2007.
[28] R. W. Schefer, "Hydrogen enrichment for improved lean flame stability," *International Journal of Hydrogen Energy,* vol. 28, pp. 1131-1141, 2003.
[29] N. Docquier and S. Candel, "Combustion control and sensors: a review," *Progress in energy and combustion science,* vol. 28, no. 2, pp. 107-150, 2002.
[30] A. S. Morgans and A. P. Dowling, "Model-based control of combustion instabilities," *Journal of Sound and Vibration,* vol. 299, no. 1-2, pp. 261-282, 2007.
[31] D. Campos-Delgado, K. Zhou, D. Allgood, and S. Acharya, "Active control of combustion instabilities using model-based controllers," *Combustion science and technology,* vol. 175, no. 1, pp. 27-53, 2003.
[32] J. Hathout, M. Fleifil, A. Annaswamy, and A. F. Ghoniem, "Combustion instability active control using periodic fuel injection," *Journal of Propulsion and Power,* vol. 18, no. 2, pp. 390-399, 2002.

[33] J.-Z. Chu, S.-S. Shieh, S.-S. Jang, C.-I. Chien, H.-P. Wan, and H.-H. Ko, "Constrained optimization of combustion in a simulated coal-fired boiler using artificial neural network model and information analysis☆," *Fuel,* vol. 82, no. 6, pp. 693-703, 2003.
[34] V. r. Havlena and J. Findejs, "Application of model predictive control to advanced combustion control," *Control Engineering Practice,* vol. 13, no. 6, pp. 671-680, 2005.
[35] B. Hu, Y. Huang, and J. Xu, "A Hybrid Semi-empirical Model for Lean Blow-Out Limit Predictions of Aero-engine Combustors," *Journal of Engineering for Gas Turbines and Power,* vol. 137, no. 3, p. 031502, 2015.
[36] A. H. Lefebvre, *Gas turbine combustion*. CRC press, 1998.
[37] R. C. Steele, J. H. Tonouchi, D. G. Nicol, D. C. Horning, P. C. Malte, and D. T. Pratt, "Characterization of NOx, N2O, and CO for lean-premixed combustion in a high-pressure jet-stirred reactor," in *ASME 1996 International Gas Turbine and Aeroengine Congress and Exhibition*, 1996, pp. V003T06A019-V003T06A019: American Society of Mechanical Engineers.
[38] P. Malte and D. Pratt, "Measurement of atomic oxygen and nitrogen oxides in jet-stirred combustion," in *Symposium (international) on combustion*, 1975, vol. 15, no. 1, pp. 1061-1070: Elsevier.
[39] G. Moréac, P. Dagaut, J. Roesler, and M. Cathonnet, "Nitric oxide interactions with hydrocarbon oxidation in a jet-stirred reactor at 10 atm," *Combustion and Flame,* vol. 145, no. 3, pp. 512-520, 2006.
[40] S. Bragg, "Application of reaction rate theory to combustion chamber analysis," AERONAUTICAL RESEARCH COUNCIL LONDON (UNITED KINGDOM)1953.
[41] J. Swithenbank, "Combustion Fundamentals," *AFOSR 70-2110 TR,* 1970.
[42] A. S. Feitelberg, V. E. Tangirala, R. A. Elliott, R. E. Pavri, and R. B. Schiefer, "Reduced NOx Diffusion Fame Combustors for Industrial Gas Turbines," *ASME Journal of Engineering for Gas Turbines and Power,* vol. 123, no. 4, pp. 757-765, 2001.
[43] K. B. Fackler, M. Karalus, I. Novosselov, J. Kramlich, P. Malte, and S. Vijlee, "NOx Behavior for Lean-Premixed Combustion of Alternative Gaseous Fuels," *Journal of Engineering for Gas Turbines and Power,* vol. 138, no. 4, p. 041504, 2016.
[44] A. Schlegel, P. Benz, T. Griffin, W. Weisenstein, and H. Bockhorn, "Catalytic Stabilization of Lean Premixed Combustion: Method for Improving NOx Emissions," *Combustion and Flame,* vol. 105, no. 3, pp. 332-340,, 1996.
[45] G. Sturgess and D. T. Shouse, "A Hybrid Model for Calculating Lean Blow-outs in Practical Combustors," *AIAA Paper,* vol. 96, no. 3125, 1996.
[46] P. M. Rubins and D. T. Pratt, "Zone Combustion Model Development and Use: Application to Emissions Control," *American Society of Mechanical Engineers, 91-JPGC-FACT-25,* vol. 91-JPGC-FACT-25, 1991.
[47] I. V. Novosselov, P. C. Malte, S. Yuan, R. Srinivasan, and J. C. Y. Lee, "Chemical Reactor Network Application to Emissions Prediction for Industrial DLE Gas Turbine," presented at the ASME Turbo Expo 2006: Power for Land, Sea, and Air, Barcelona, Spain, May 8 - 11, 2006, 2006.
[48] V. Fichet, M. Kanniche, P. Plion, and O. Gicquel, "A reactor network model for predicting NOx emissions in gas turbines," *Fuel,* vol. 89, no. 9, pp. 2202-2210, 9// 2010.
[49] S. Lyra and R. S. Cant, "Analysis of high pressure premixed flames using Equivalent Reactor Networks for predicting NOx emissions," *Fuel,* vol. 107, pp. 261-268, 5// 2013.

[50] I. R. Sigfrid, R. Whiddon, R. Collin, and J. Klingmann, "Influence of reactive species on the lean blowout limit of an industrial DLE gas turbine burner," *Combustion and Flame,* vol. 161, no. 5, pp. 1365-1373, 2014.
[51] G. Sturgess, "Combustor LBO Design Model Evaluation," PRATT AND WHITNEY WEST PALM BEACH FL GOVERNMENT ENGINES AND SPACE PROPULSION1995.
[52] M. F. Karalus, "An investigation of lean blowout of gaseous fuel alternatives to natural gas," 2014.
[53] R. J. Robertus, K. L. Nielsen, C. T. Crowe, and D. T. Pratt, "Attempt To Reduce Nox Emissions From Pulverized Coal Furnaces," *Environmental Science and Technology,* vol. 9, no. 9, pp. 859-862, 1975.
[54] D. Benedetto, S. Pasini, M. Falcitelli, C. La Marca, and L. Tognotti, "NOx emission prediction from 3-D complete modelling to reactor network analysis," *Combustion Science and Technology,* vol. 153, no. 1, pp. 279-294, 2000.
[55] T. Faravelli, L. Bua, A. Frassoldati, A. Antifora, L. Tognotti, and E. Ranzi, "A new procedure for predicting NOx emissions from furnaces," " *Computers & Chemical Engineering, v* vol. 25, n, no. 4-6, pp. , pp. 613-18, , 2001.
[56] M. Falcitelli, S. Pasini, N. Rossi, and L. Tognotti, "CFD + reactor network analysis: an integrated methodology for the modeling and optimization of industrial systems for energy saving and pollution reduction," *Applied Thermal Engineering,* vol. 22, pp. 971–979, 2002.
[57] E. Ranzi, S. Pierucci, P. C. Aliprandi, and S. Stringa, "Comprehensive and detailed kinetic model of a traveling grate combustor of biomass," *Energy & Fuels,* vol. 25, no. 9, pp. 4195-4205, 2011.
[58] D. T. Pratt and J. D. Wormeck, "CREK, Combustion Reaction Equilibrium and Kinetics in Laminar and Turbulent Flows," *Report TEL-76-1, Department of Mechanical Engineering, Washington State University, Pullman, WA,* 1976.
[59] D. T. Pratt and K. Radhakrishnan, "CREK1D: A computer code for transient, gas-phase combustion kinetics," *NASA Technical Memorandum,* 1984.
[60] K. Radhakrishnan and D. T. Pratt, "Fast Algorithm for Calculating Chemical Kinetics in Turbulent Reacting Flows," *Comb. Sci. Tech.,* pp. 155-176, 1988.
[61] D. T. Pratt, "Calculation of Chemically Reactive Flows with Complex chemistry," *in Studies in Convection, B.E. Launder, Editor, Academic Press,* vol. 2, 1997.
[62] I. Novosselov, P. Malte, S. Yuan, R. Srinivasan, and J. Lee, "Chemical reactor network application to emissions prediction for industial dle gas turbine," in *ASME turbo expo 2006: Power for land, sea, and air*, 2006, pp. 221-235: American Society of Mechanical Engineers.
[63] I. V. Novosselov, "Chemical reactor networks for combustion systems modeling," Ph.D Disseration, Department of Mechanical Engineering, University of Washington, 2006.
[64] M. F. Karalus, "An investigation of lean blowout of gaseous fuel alternatives to natural gas," Ph.D Dissertation Department of Mechanical Engineering, University of Washington, 2014.
[65] D. G. Nicol, "The Chemical Reactor Model Combustion Code," *Section 4.6 in Mellor, A.M., Editor. "NOx and CO Emissions Models for Gas-Fired, Lean Premixed Combustion Turbine: Final Report," Vanderbilt University, Nashville, TN,* 1996.

[66] J.-Y. Ren, W. Qin, F. Egolfopoulos, H. Mak, and T. Tsotsis, "Methane reforming and its potential effect on the efficiency and pollutant emissions of lean methane–air combustion," *Chemical Engineering Science,* vol. 56, no. 4, pp. 1541-1549, 2001.

[67] J.-Y. Ren, W. Qin, F. Egolfopoulos, and T. Tsotsis, "Strain-rate effects on hydrogen-enhanced lean premixed combustion," *Combustion and Flame,* vol. 124, no. 4, pp. 717-720, 2001.

[68] E. Sher and S. Refael, "A simplified reaction scheme for the combustion of hydrogen enriched methane/air flame," *Combustion science and technology,* vol. 59, no. 4-6, pp. 371-389, 1988.

[69] V. Di Sarli and A. Di Benedetto, "Laminar burning velocity of hydrogen–methane/air premixed flames," *International Journal of Hydrogen Energy,* vol. 32, no. 5, pp. 637-646, 2007.

[70] C. Safta and C. Madnia, "Autoignition and structure of nonpremixed CH 4/H 2 flames: detailed and reduced kinetic models," *Combustion and flame,* vol. 144, no. 1, pp. 64-73, 2006.

[71] N. Chaumeix, S. Pichon, F. Lafosse, and C.-E. Paillard, "Role of chemical kinetics on the detonation properties of hydrogen/natural gas/air mixtures," *International Journal of Hydrogen Energy,* vol. 32, no. 13, pp. 2216-2226, 2007.

[72] J. C. Y. Lee, "Reduction of NOx emission for lean prevaporized-premixed combustors," Ph.D Dissertation Department of Mechanical Engineering, University of Washington, 2000.

Appendix I. Igniter

For initially igniting the reactor (with hydrogen), an electric arc based ignitor is used. The ignitor consists of two tungsten electrodes, which are encased in a ceramic tube with separate holes for each electrode. This tube renders support to the electrodes apart from protecting them from the high-temperature environment to which they are exposed inside the reactor. One of the electrodes is connected to a Webster ignition transformer (Primary: 120V/8.5A, Secondary: 8.5kV/20mA) via copper wire and the other electrode is grounded to complete the circuit. At the other end of the tube, the electrodes are kept extended out to a length of ~0.75mm. This length is ideal for the production of the desired arc since a higher length would result in a diffused arc and would not serve the purpose. Similarly, the gap between the electrodes needs to be ~1mm as a greater gap may not produce an arc at all. Also, to ensure that the current has only one path to flow, which is at the tip of the electrodes, the junction between the tungsten electrodes and the copper wires are coated with an epoxy resin.

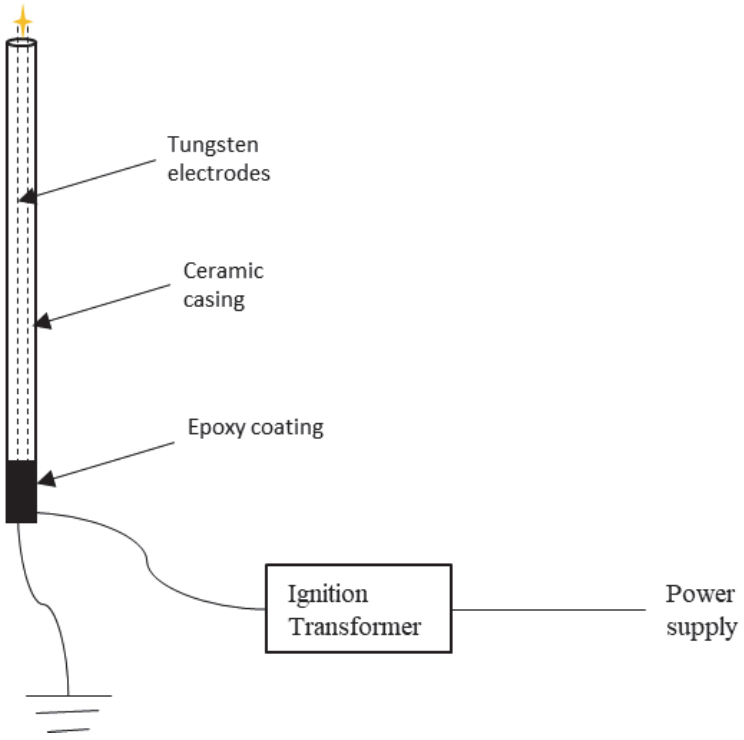

Figure A.1: Schematic for Ignitor

Appendix II. Standard Experimental Procedure

Initial setup

1. Open the garage door for ease of access.
2. Set up the controller station
   (a) Ensure that the ribbon wires from MyRio Control box to the Fuel and Air Mass Flow Controllers are connected properly.
   (b) Connect the USB cables from the MyRio and TC-DAQ with the user laptop.
   (c) Confirm that the power source to the MyRio and batteries are running.
   (d) Open the following LabVIEW project file:-
   C:\Users\David\Desktop\JSR Operate.lvproj
   (e) Run the following VI to establish the interface between the MyRio block and LabVIEW:-
   UWNRG-myRIO-1900-030b4666 (172.22.11.2)\Main_MyRIO.vi
   (f) Run the following VI to establish the interface between the TCDAQ and LabVIEW:-
   My Computer\USB_TC-08.vi

   Select the channel based on the channel being used on the TCDAQ and set it to R-type

   (g) Run the following VI to enter the User control screen:-
   My Computer\Main_MyComp.vi

3. Set up the air flow
   (a) Close the bypass valve to the rotameter, so that rotameter is in series with the air MFC.
   (b) Open the air outlet valve to the premixer completely.
   (c) Set the air pressure regulator at 50 psig.
   (d) Ensure air flow through the reactor by giving random airflow setpoint in Manual air flow control mode. Also, confirm the flow feedback value.

4. Set up fuel flow
    (a) Open the outlet valves for hydrogen and methane cylinders. Ensure if adequate pressure
    (b) Adjust the cylinder outlet pressure regulators to obtain pressures of 30 psig for hydrogen and 50 psig for methane on the rig
    (c) Open the methane inlet/ outlet valves, hydrogen inlet valve and fuel inlet to reactor valve.
    (d) Check the flow of hydrogen through the reactor by slightly opening and closing the manual control valve.
    (e) Check the same for methane using the fuel MFC.
    (f) Once fuel flows are confirmed, keep all fuel valves on the rig closed until ready for ignition.

5. Set up thermocouple
    (a) Insert the thermocouple into the reactor and move to the center of the reactor. This can be confirmed visually from side port; there should be an audible difference caused by the thermocouple interfering with the jet. Note the reading on the scale at the bottom of the thermocouple holder.
    (b) Move the thermocouple outwards such that the tip is positioned at a distance of 9 mm from center
    (c) Secure in place with the plastic screw

6. Check ignitor
    (a) Ensure that the wire connecting the ignitor to the ignition transformer is secure
    (b) Plug in the ignition transformer
    (c) Switch on the ignitor (using the metal switch on the bottom right of the rig). A spark should be visible.
    (d) Switch off the ignitor.

Ignition and Warm-up

1. Set the Air Control Mode to 'Manual' and set the Air Flow Rate to 40 LPM.
2. Insert the ignitor into the reactor until an audible confirmation of the ignitor tip interacting with the air jet is heard.
3. Turn on the ignitor. Ensure the spark from the open port on the front side of the reactor.
4. Open the fuel inlet to reactor and hydrogen inlet valves.
5. Slowly increase hydrogen flow using the control valve until a pop is heard. Keep increasing the hydrogen flow until reactor temperature reaches 1100-1200° C.
6. Allow the reactor to warm up to a temperature of ~1350° C.
7. Set the Control Type to 'Control Air and Phi' and switch on the "Methane Fuel On' control.
8. Open the methane inlet and outlet valves.
9. Slowly increase the Phi to the desired experimental initial value (0.75, for the experiments in this research), starting at 0.15, in steps of 0.05. Simultaneously, decrease the hydrogen flow into the reactor so as to maintain the reactor temperature steady.
10. Once, hydrogen control valve is completely closed, also shut off the hydrogen inlet valve.
11. Gradually increase the airflow (in steps of 1 LPM) to the desired initial air flow rate.
12. Allow the reactor to warm up until the temperature stabilizes.

Setup for all combustion control experiments

1. Switch the Control Type to 'Control Air and Fuel.' Confirm if the fuel flow feedback stays the same as before.
2. Run the following VI:

   My Computer\CRN_CTRL.vi
3. Make a note of the location of the measurement file or change to the desired location.
4. Set the 'Auto Control' switch to ON. The algorithm shall now be able to control the fuel flow.

Experiment set# 1

1. Manually change the Air Flow Rate to the desired final value. The control algorithm should automatically start making changes to the fuel flow as soon as the need arises.

Experiment set# 2

1. Enter the High and Low limits and the desired ramp time. Ensure that the low limit is the same as the running air flow rate.
2. Set the 'Start' switch to ON position.

Appendix III. Data from Additional cases

This section exhibits the data from all experimental cases apart from the ones included in the main content. The behavior for all cases remains similar to that explained in Section 6.2.

1. Experiment Set# 1, Case# 1: Step Air flow increase from 0.8 g/s to 1.0 g/s

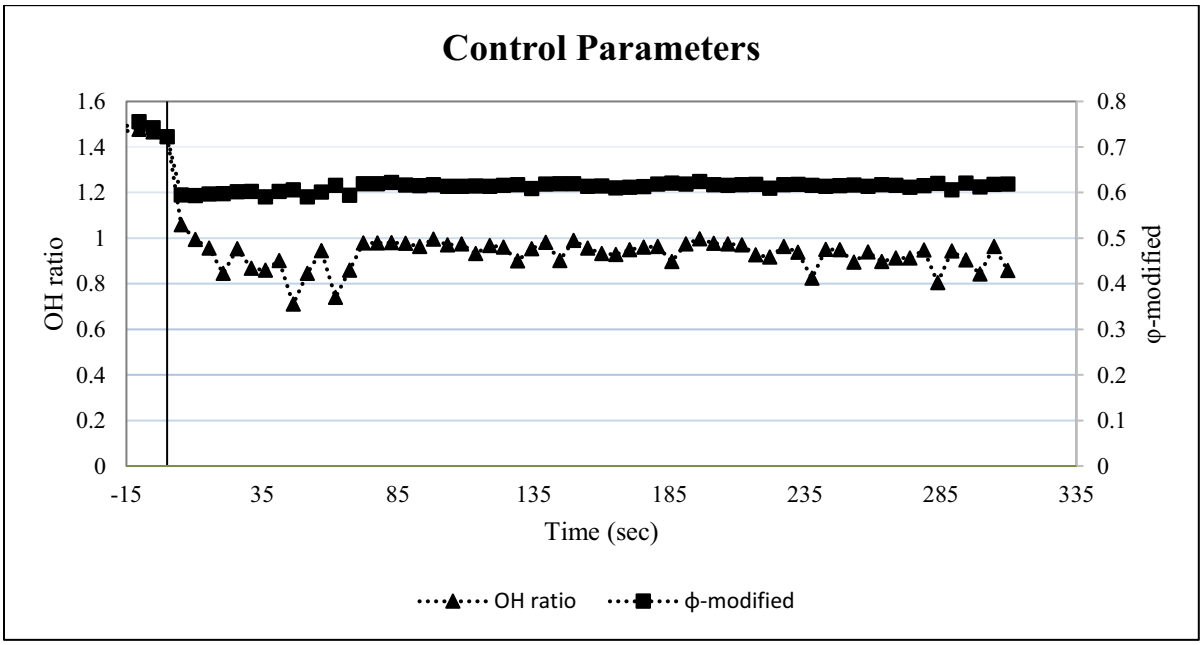

Figure A.2: Time variation of control parameters for Experiment set# 1, Case# 1

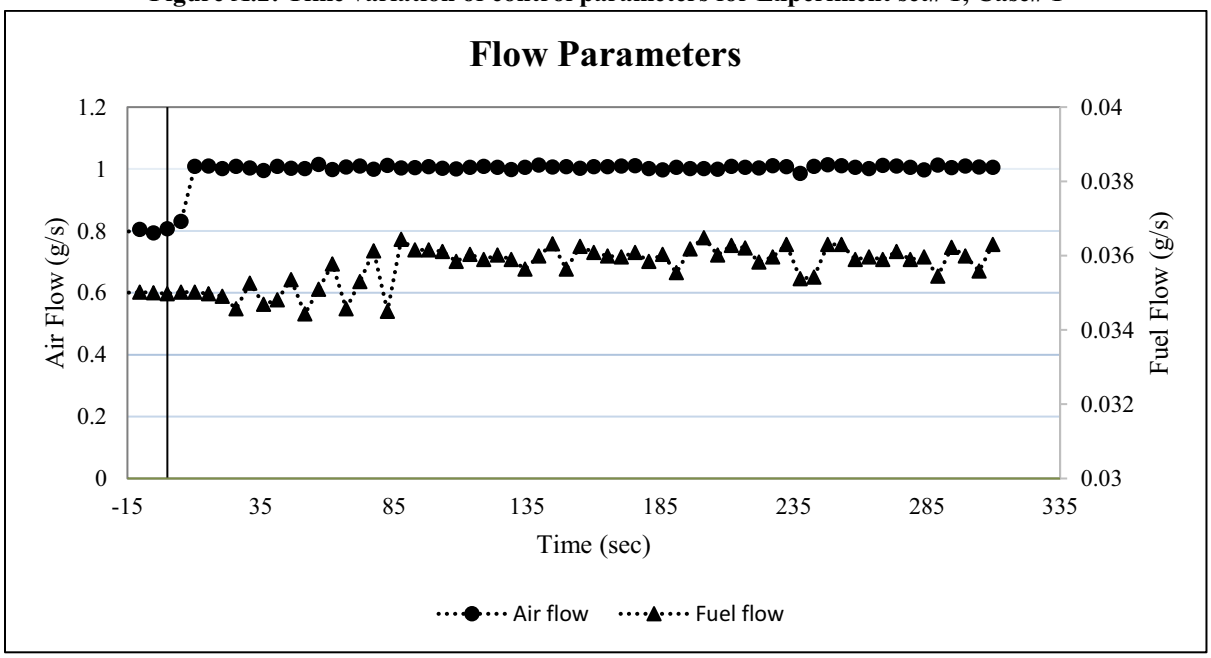

Figure A.3: Time variation of flow data for Experiment set# 1, Case# 1

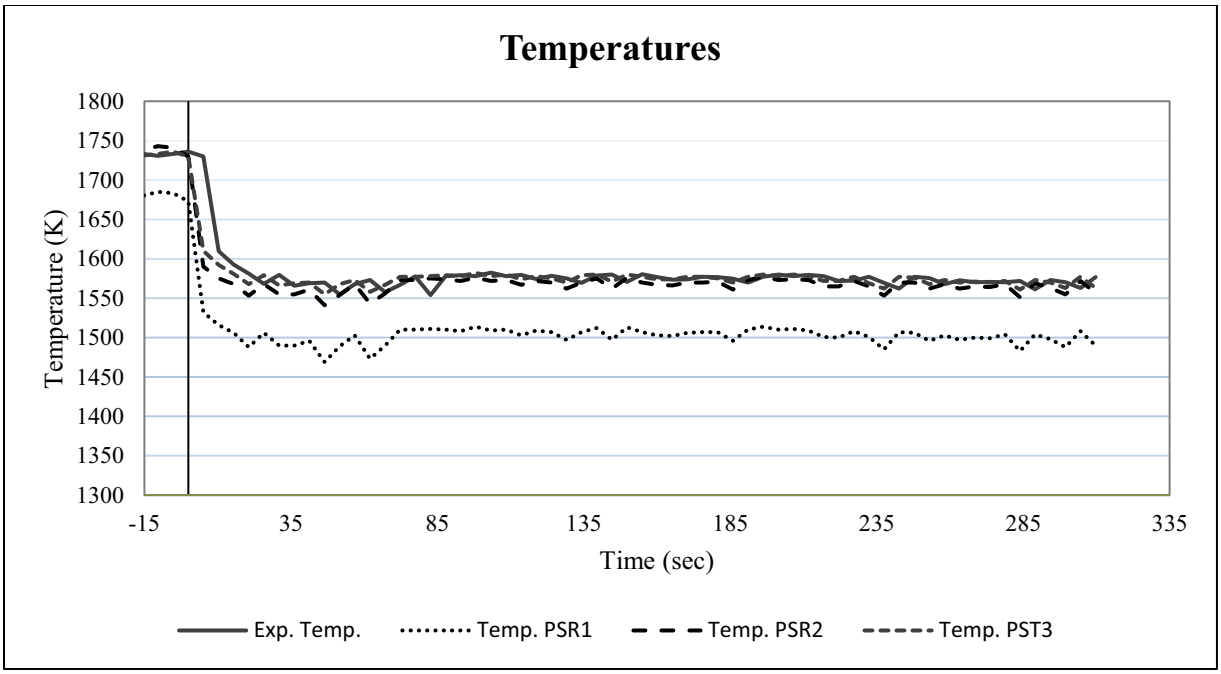

Figure A.4: Time variation of Temperatures (measured and computed) for Experiment set# 1, Case# 1

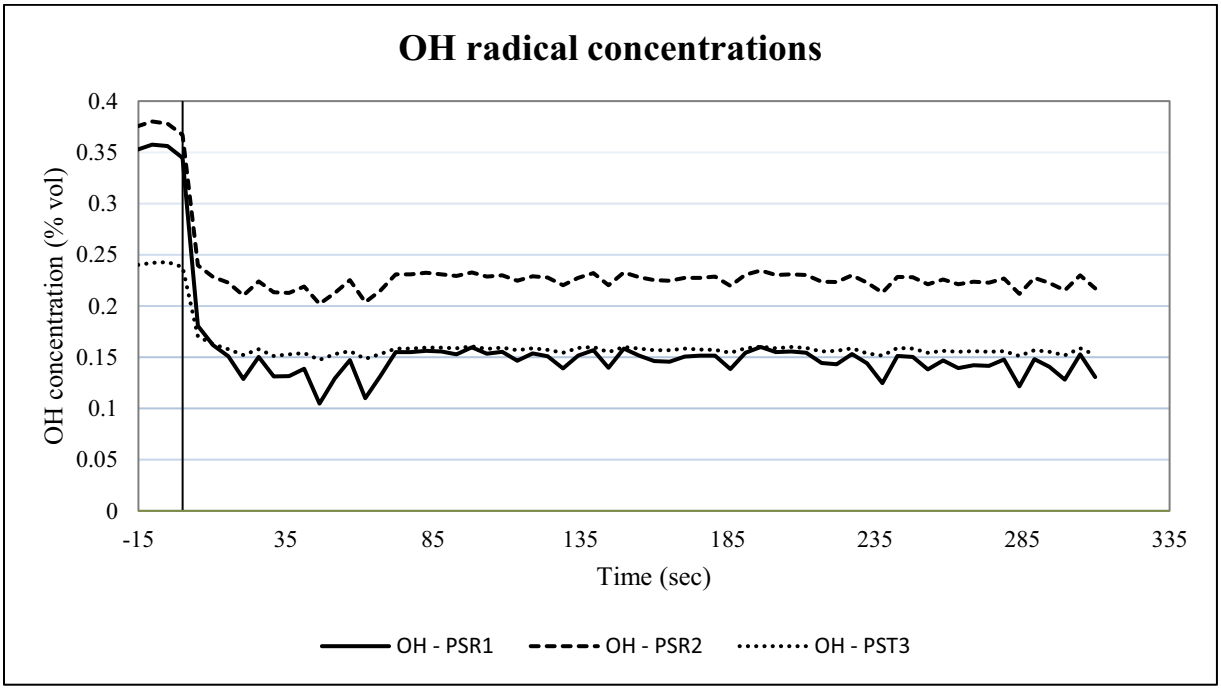

Figure A.5: Time variation of computed OH concentrations for Experiment set# 1, Case# 1

2. Experiment Set# 1, Case# 2: Step Air flow increase from 0.8 g/s to 1.1 g/s

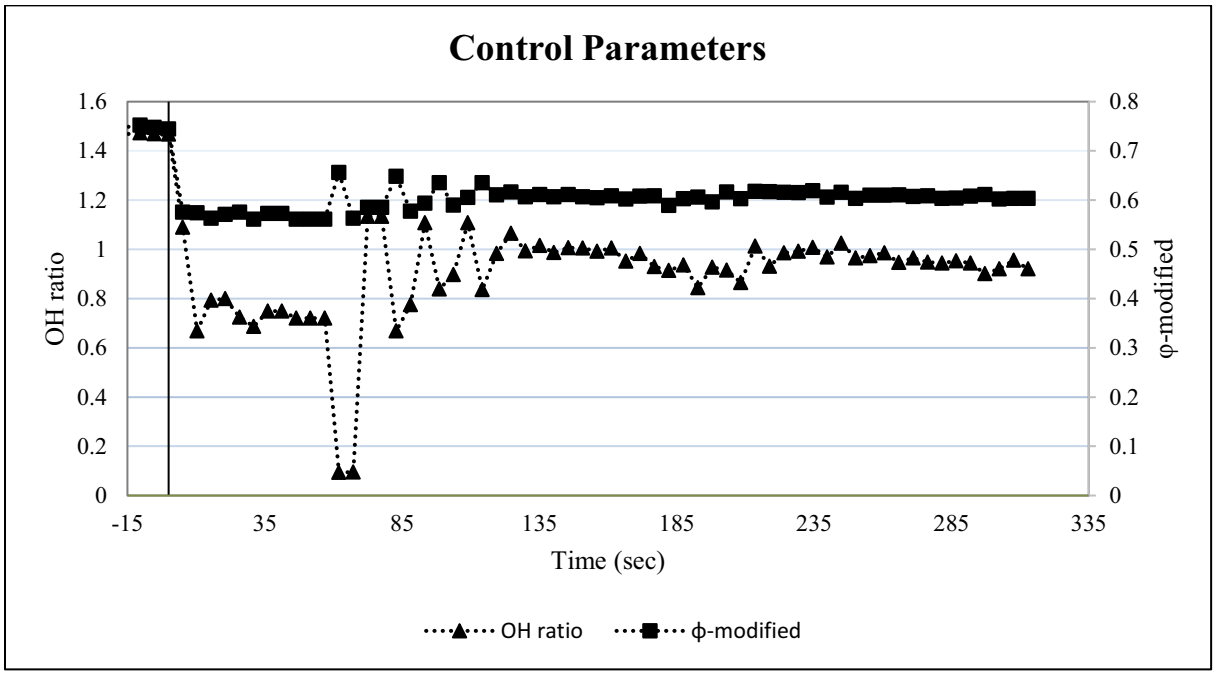

Figure A.6: Time variation of control parameters for Experiment set# 1, Case# 2

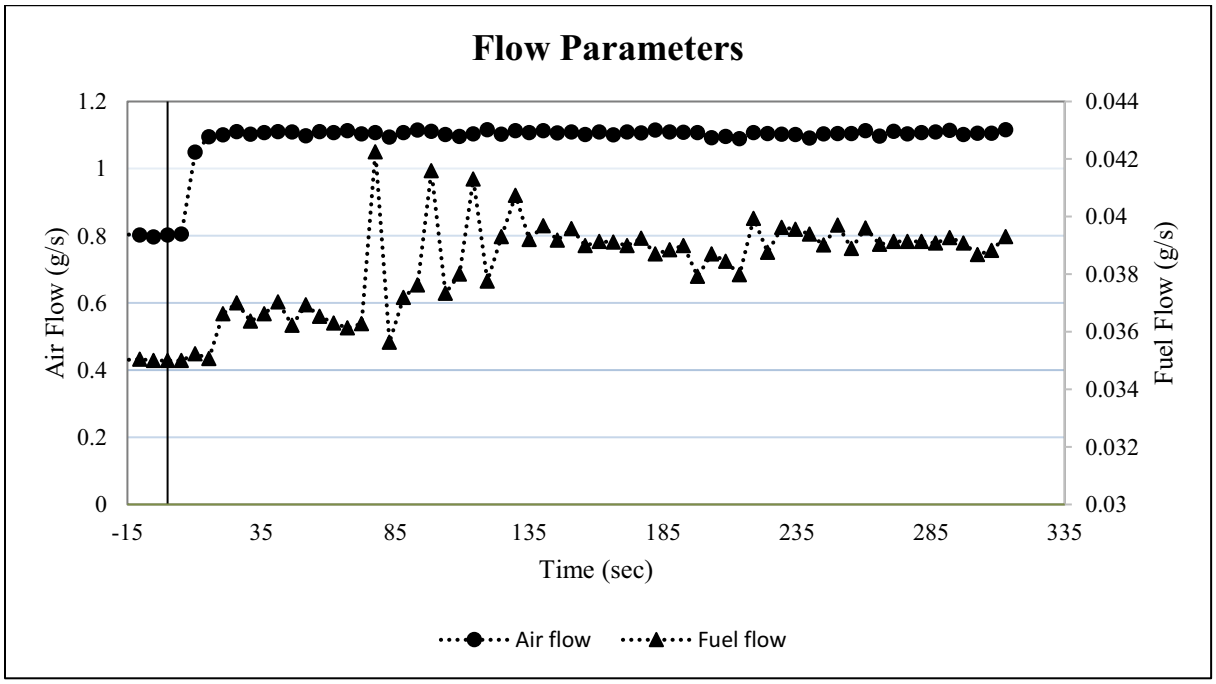

Figure A.7: Time variation of flow data for Experiment set# 1, Case# 2

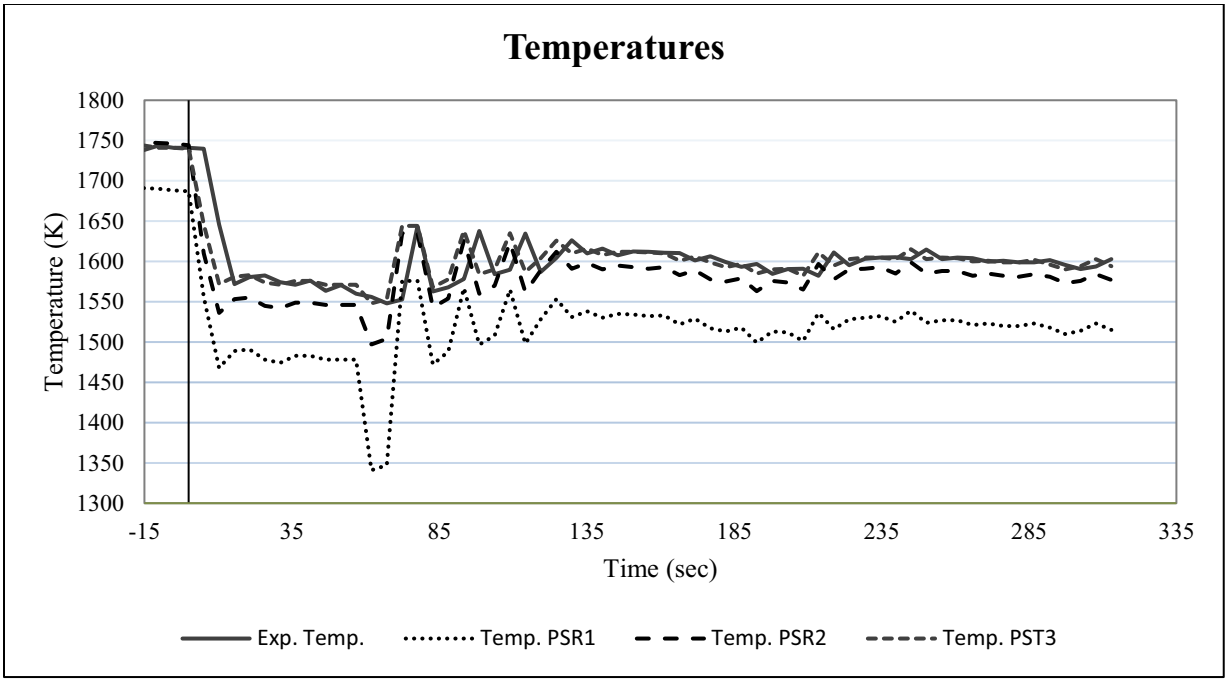

Figure A.8: Time variation of Temperatures (measured and computed) for Experiment set# 1, Case# 2

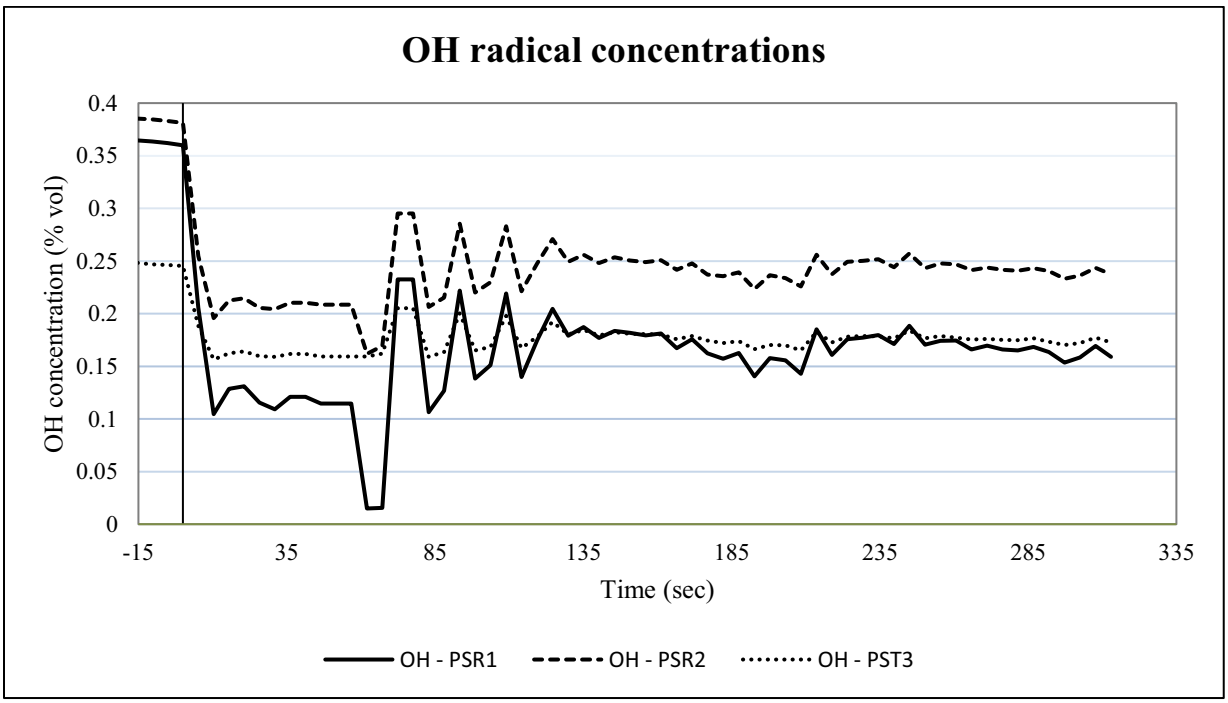

Figure A.9: Time variation of computed OH concentrations for Experiment set# 1, Case# 2

3. Experiment Set# 1, Case# 4: Step Air flow increase from 0.8 g/s to 1.3 g/s

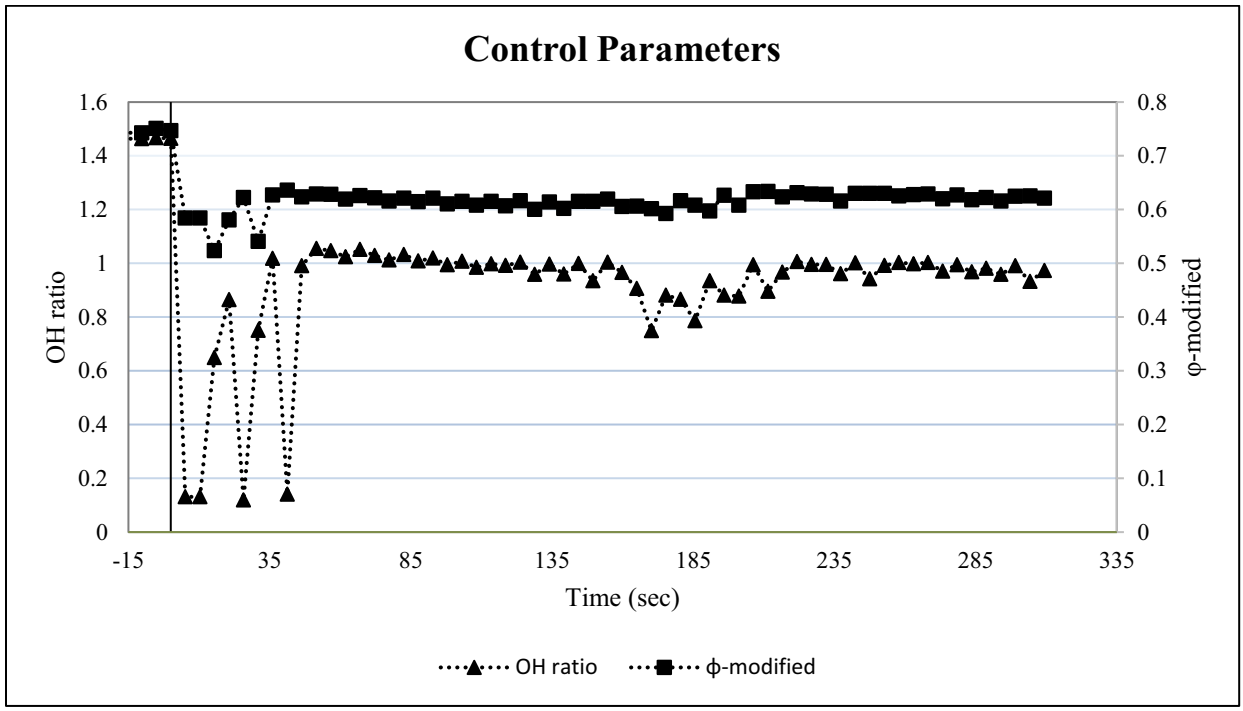

Figure A.10: Time variation of control parameters for Experiment set# 1, Case# 4

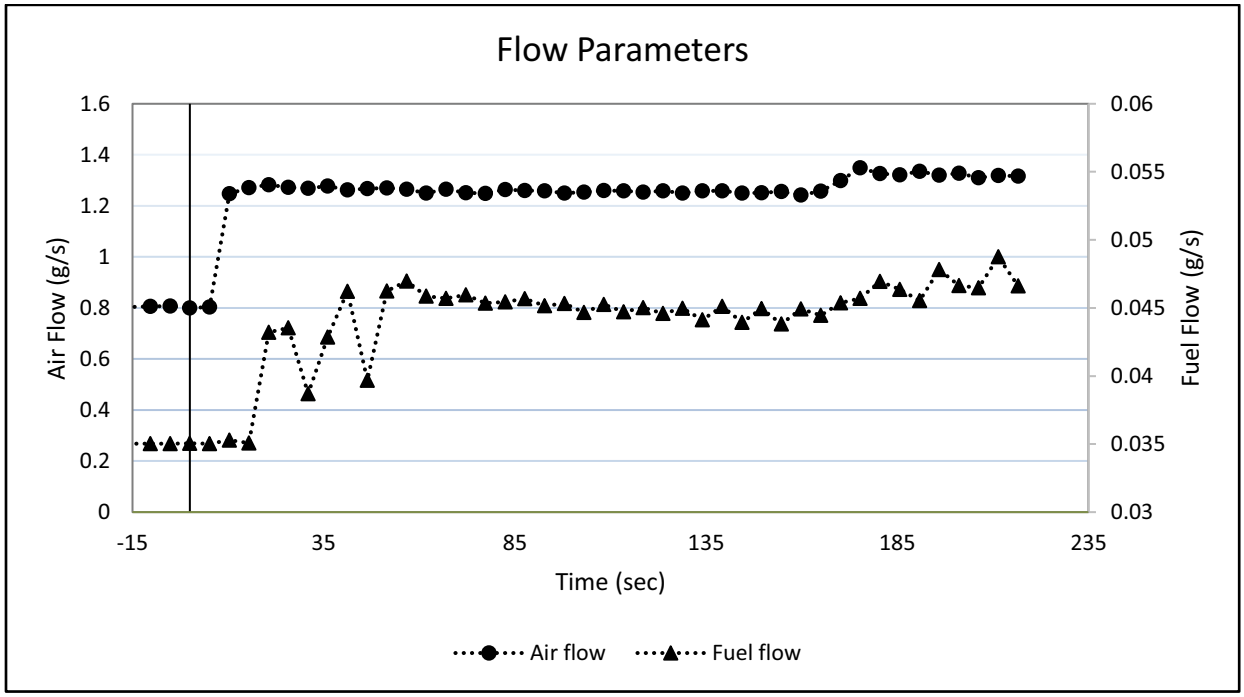

Figure A.11: Time variation of flow data for Experiment set# 1, Case# 4

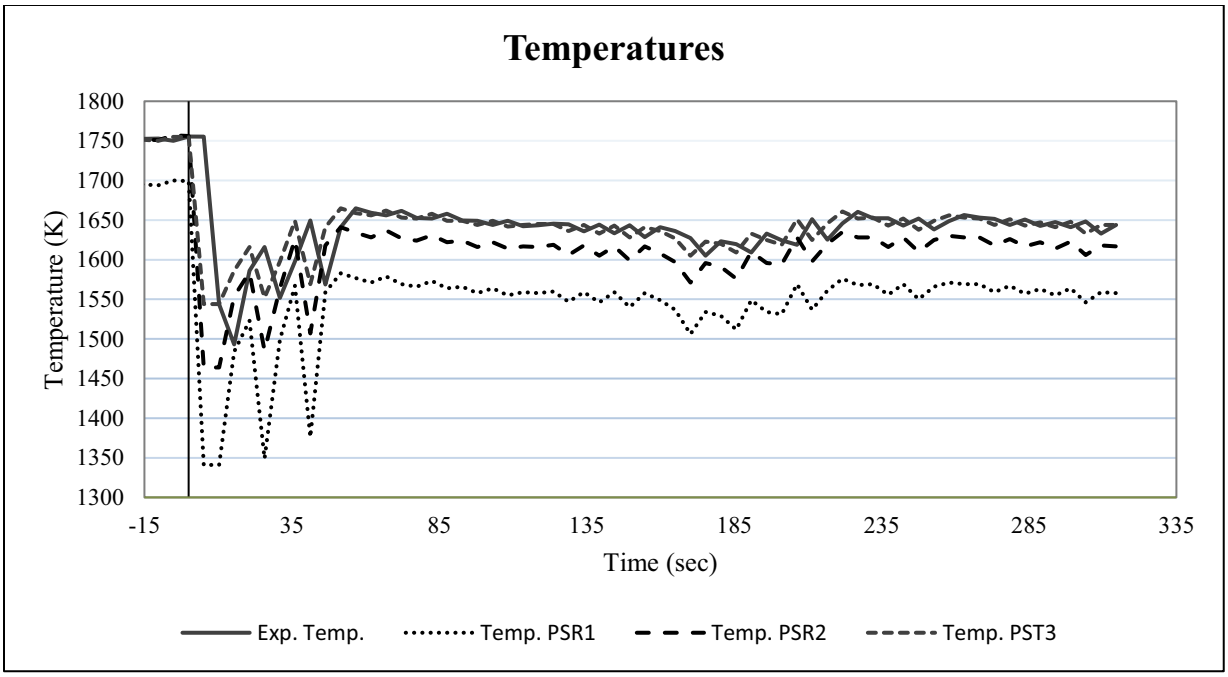

Figure A.12: Time variation of Temperatures (measured and computed) for Experiment set# 1, Case# 4

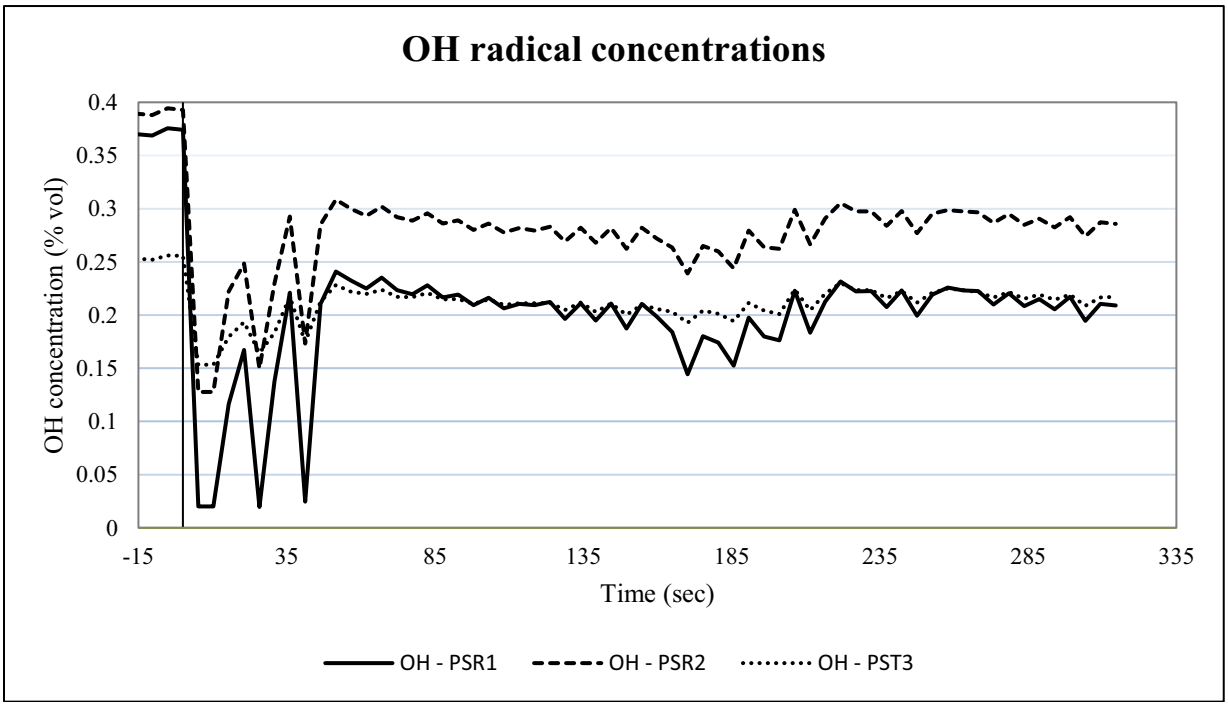

Figure A.13: Time variation of computed OH concentrations for Experiment set# 1, Case# 4

4. Experiment Set# 1, Case# 1: Gradual Air flow increase from 0.8 g/s to 1.2 g/s in 360 seconds

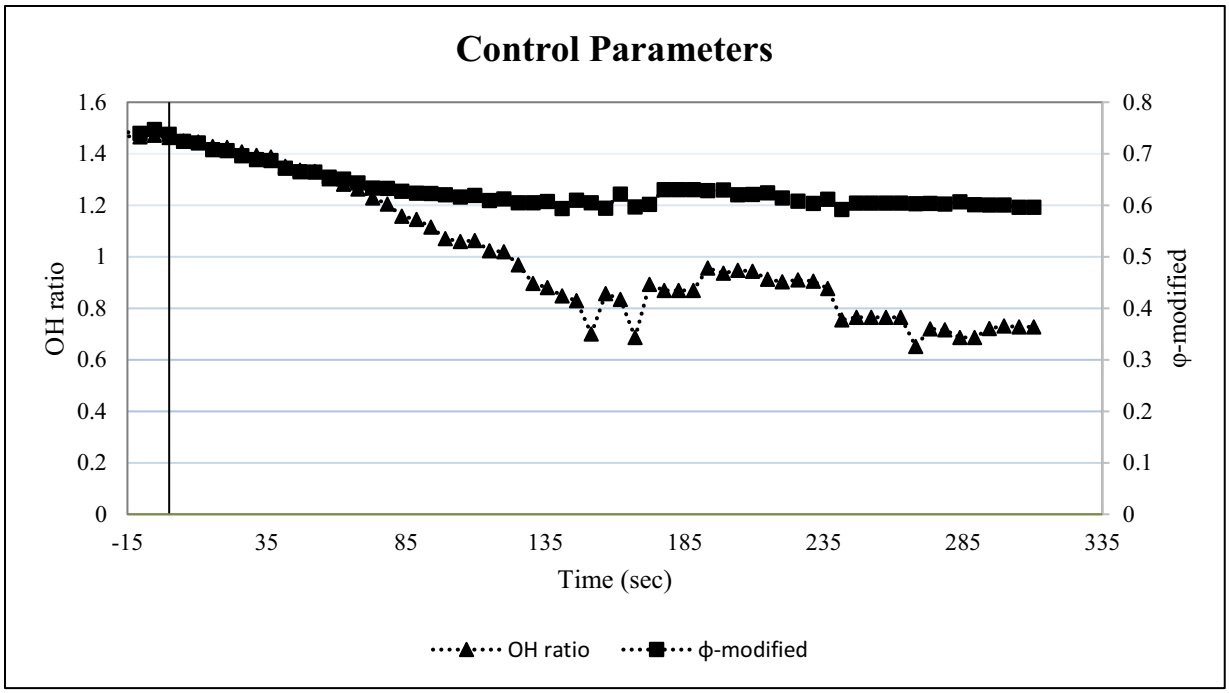

Figure A.14: Time variation of control parameters for Experiment set# 2, Case# 1

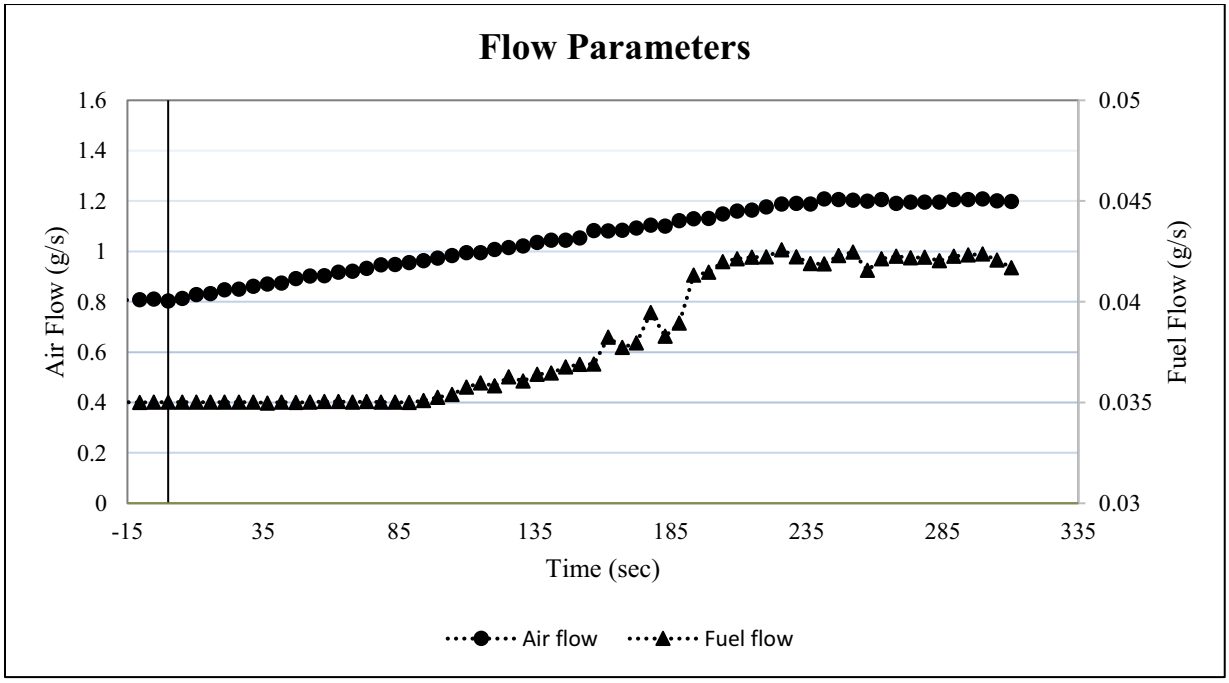

Figure A.15: Time variation of flow data for Experiment set# 2, Case# 1

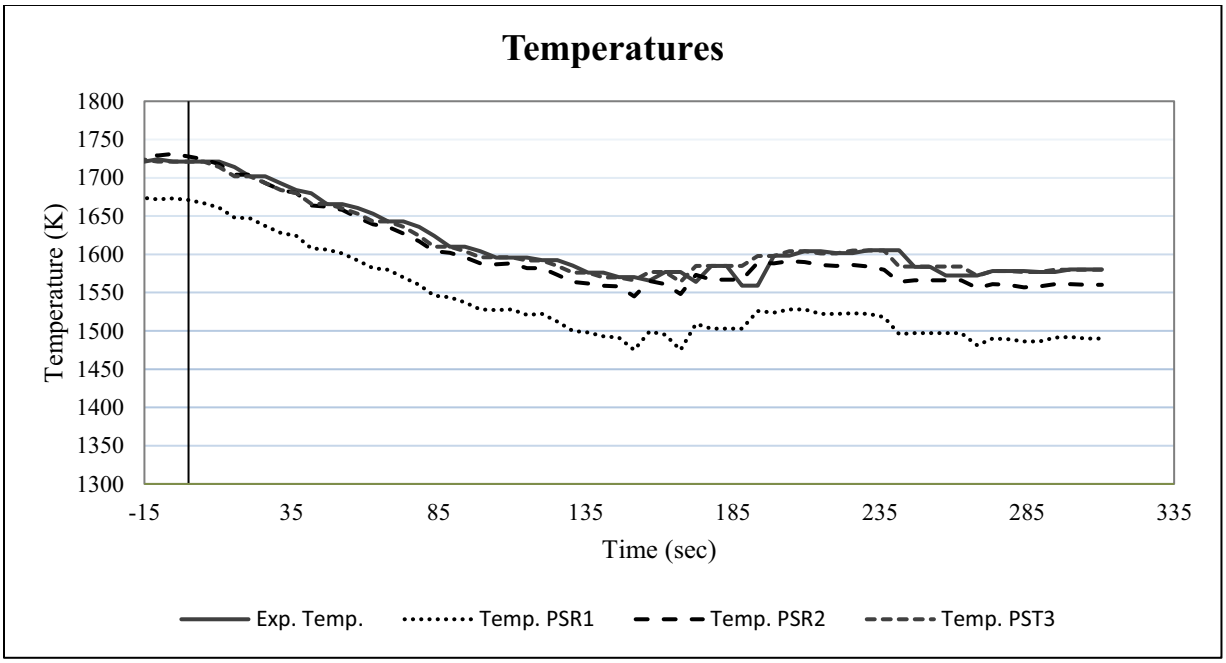

Figure A.16: Time variation of Temperatures (measured and computed) for Experiment set# 2, Case# 1

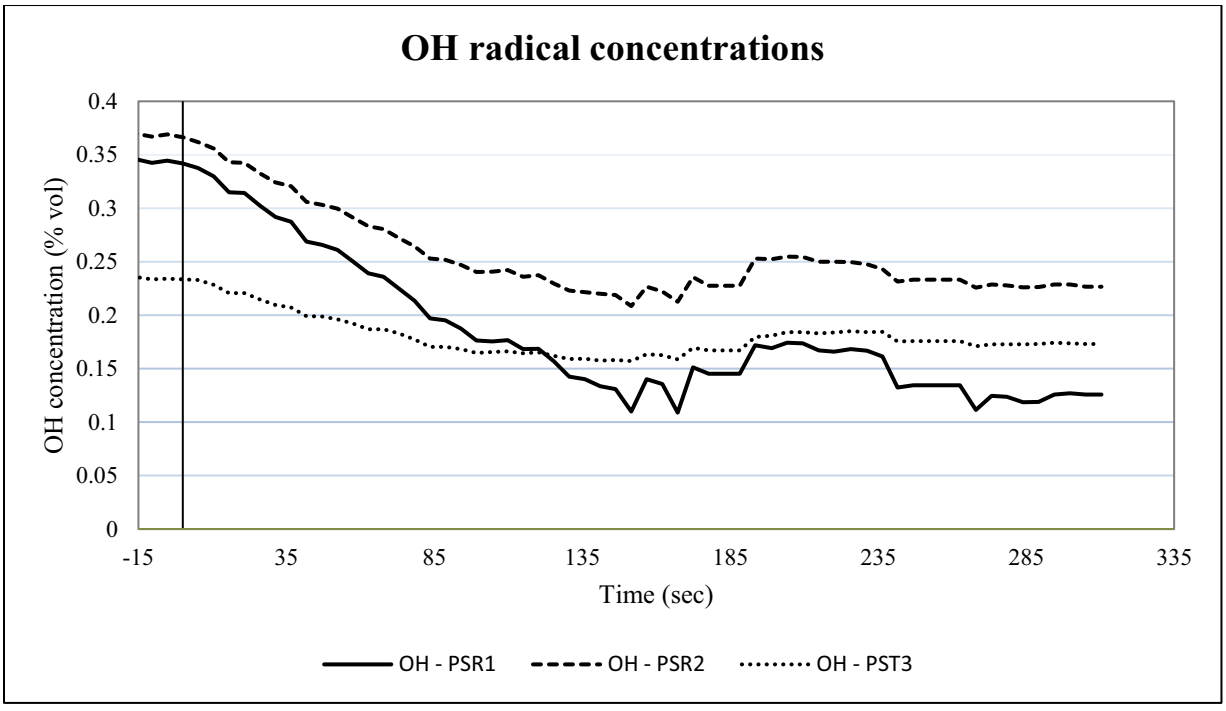

Figure A.17: Time variation of computed OH concentrations for Experiment set# 2, Case# 1

5. Experiment Set# 1, Case# 1: Gradual Air flow increase from 0.8 g/s to 1.2 g/s in 240 seconds

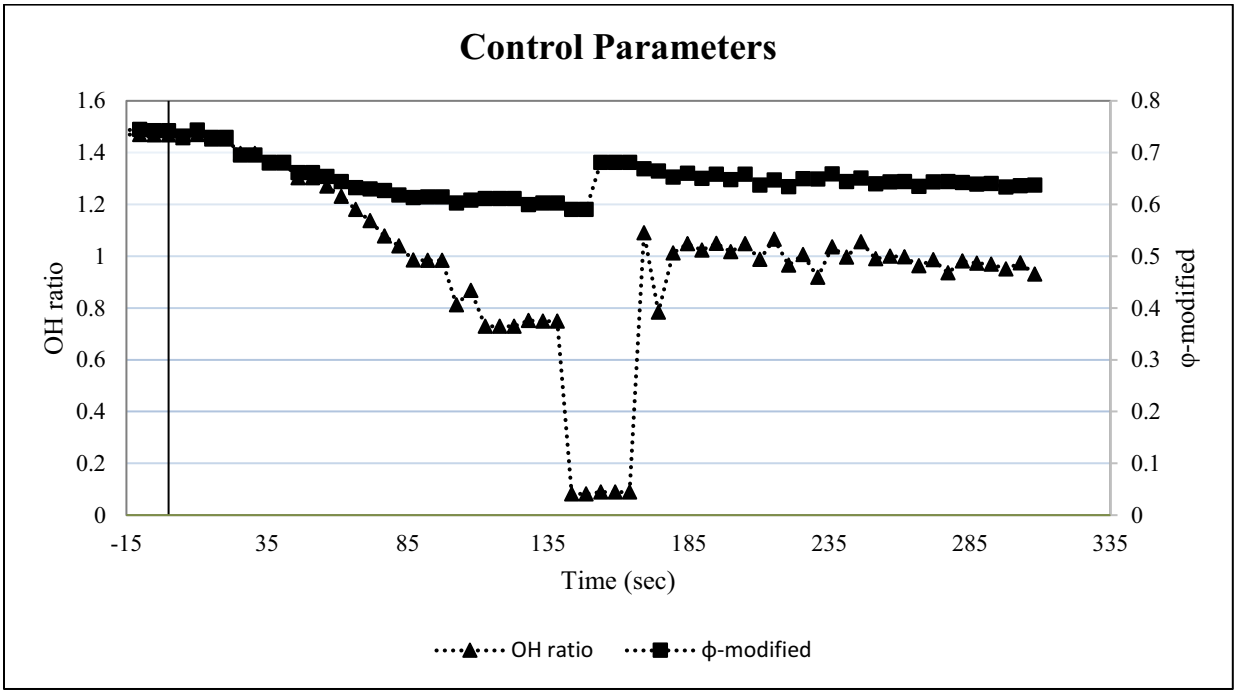

Figure A.18: Time variation of control parameters for Experiment set# 2, Case# 2

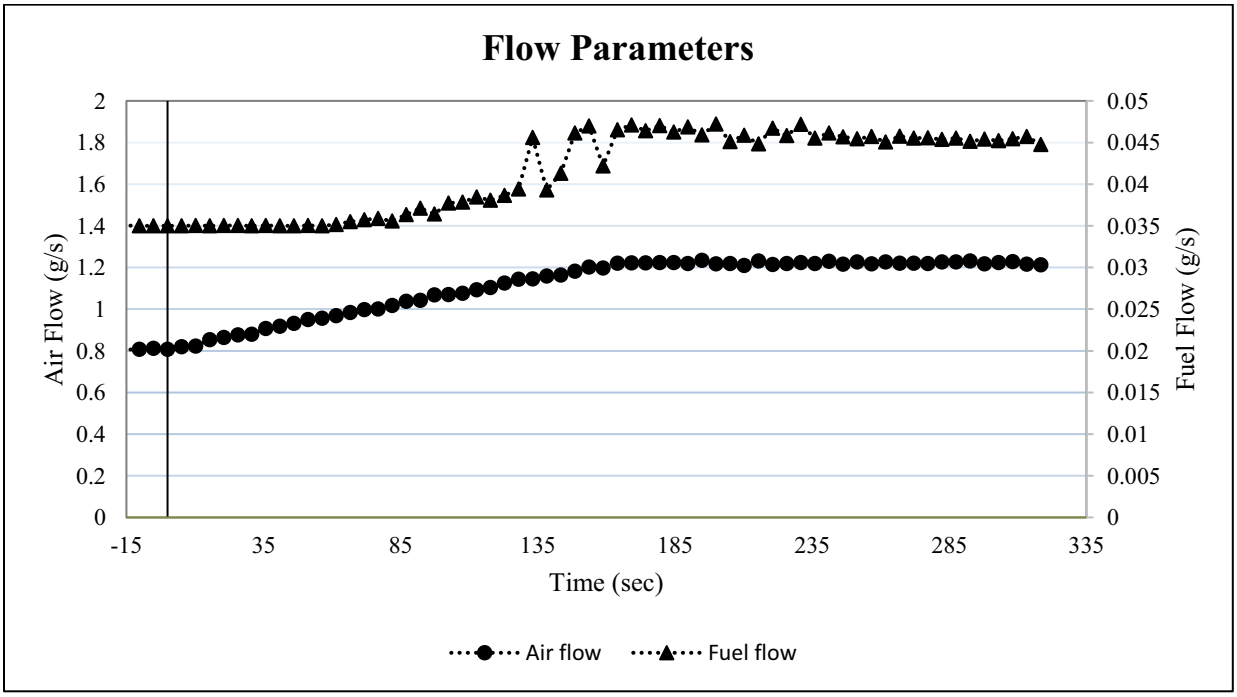

Figure A.19: Time variation of flow data for Experiment set# 2, Case# 2

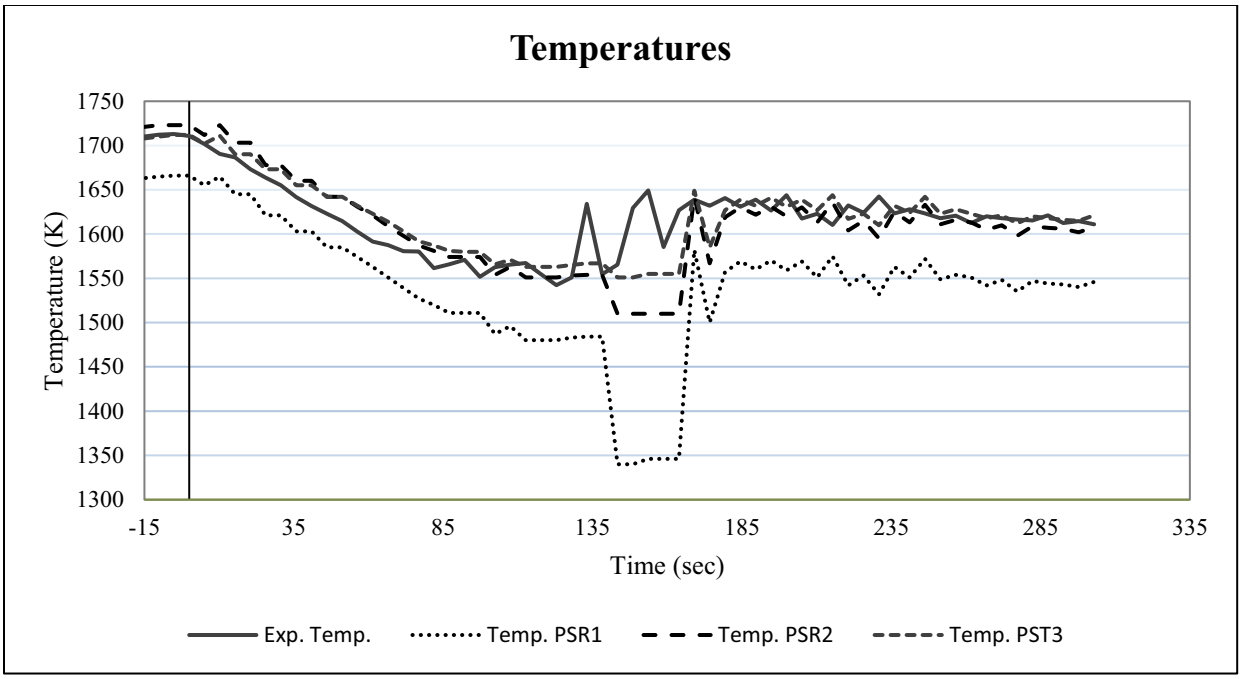

Figure A.20: Time variation of Temperatures (measured and computed) for Experiment set# 2, Case# 2

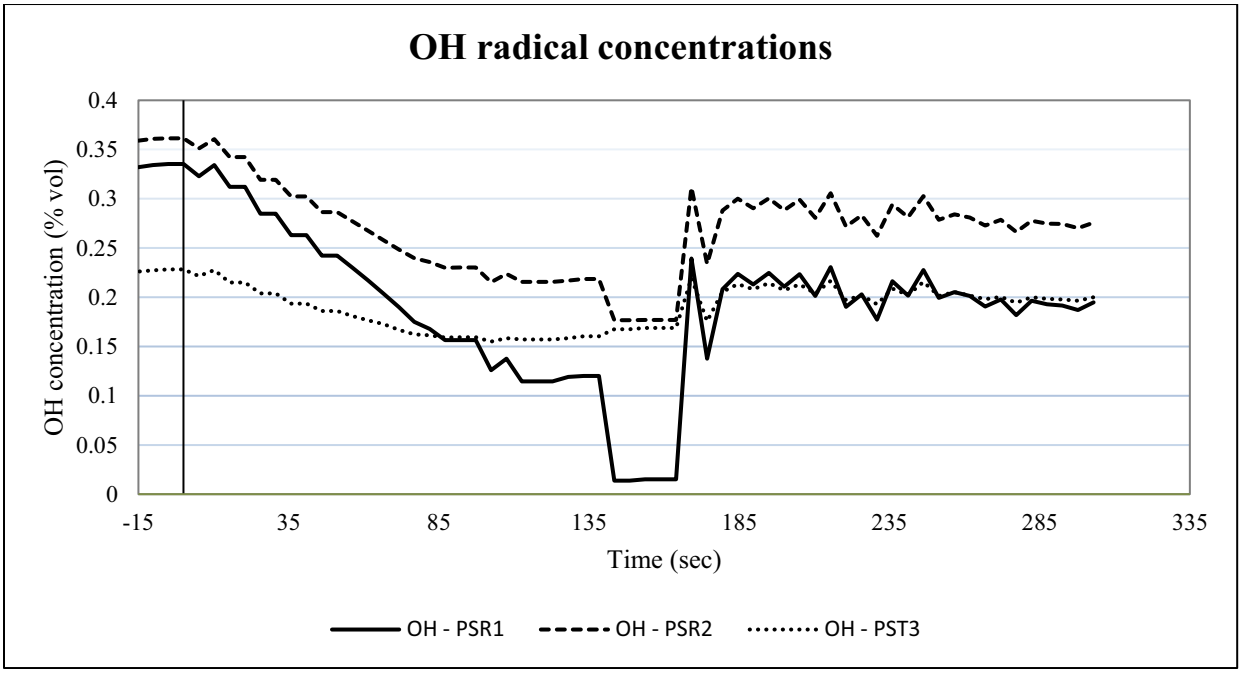

Figure A.21: Time variation of computed OH concentrations for Experiment set# 2, Case# 2

6. Experiment Set# 1, Case# 1: Gradual Air flow increase from 0.8 g/s to 1.2 g/s in 180 seconds

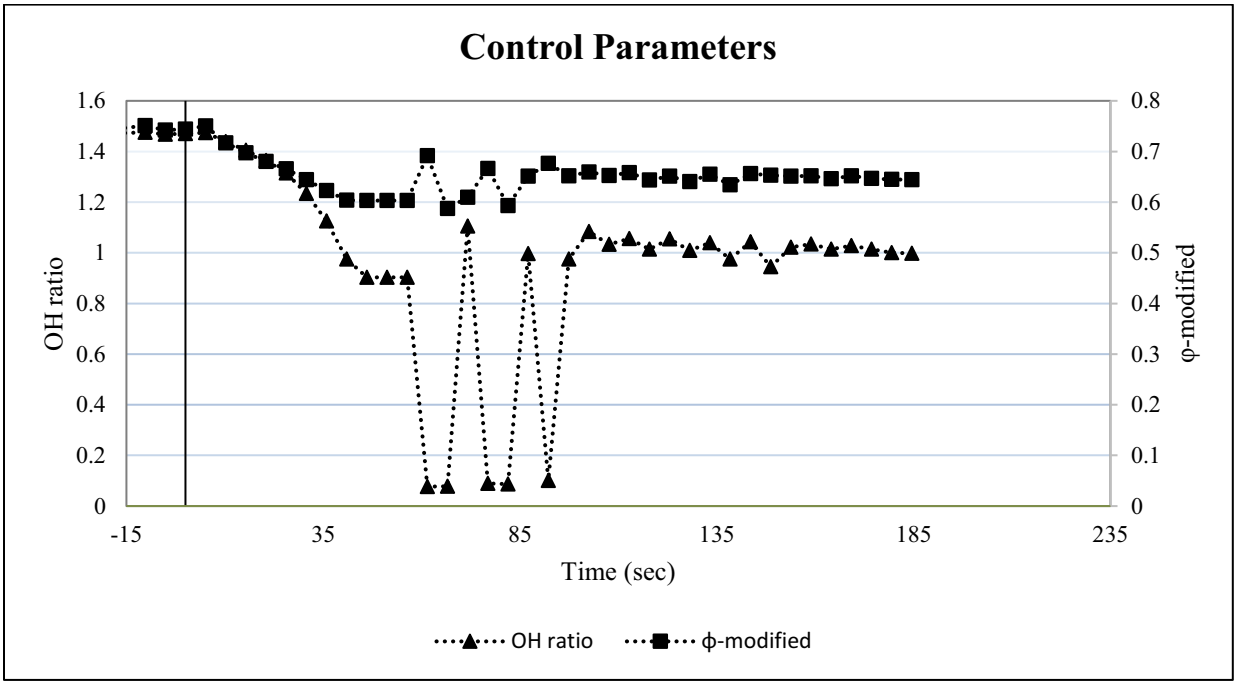

Figure A.22: Time variation of control parameters for Experiment set# 2, Case# 4

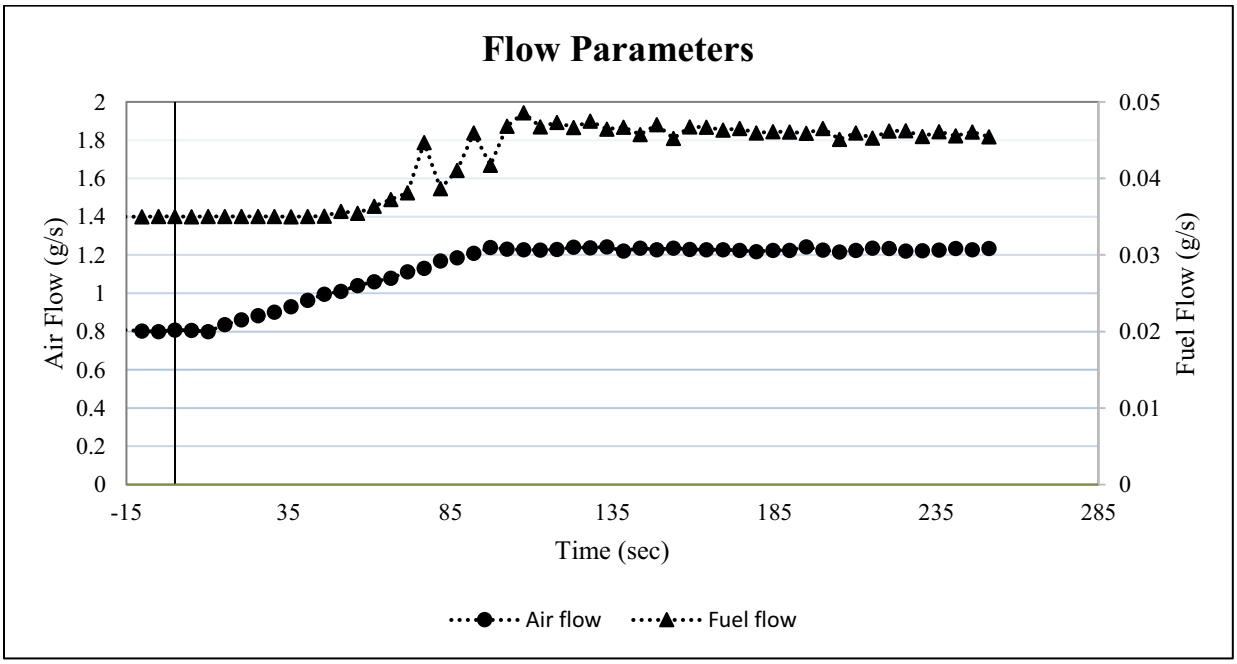

Figure A.23: Time variation of flow data for Experiment set# 2, Case# 4

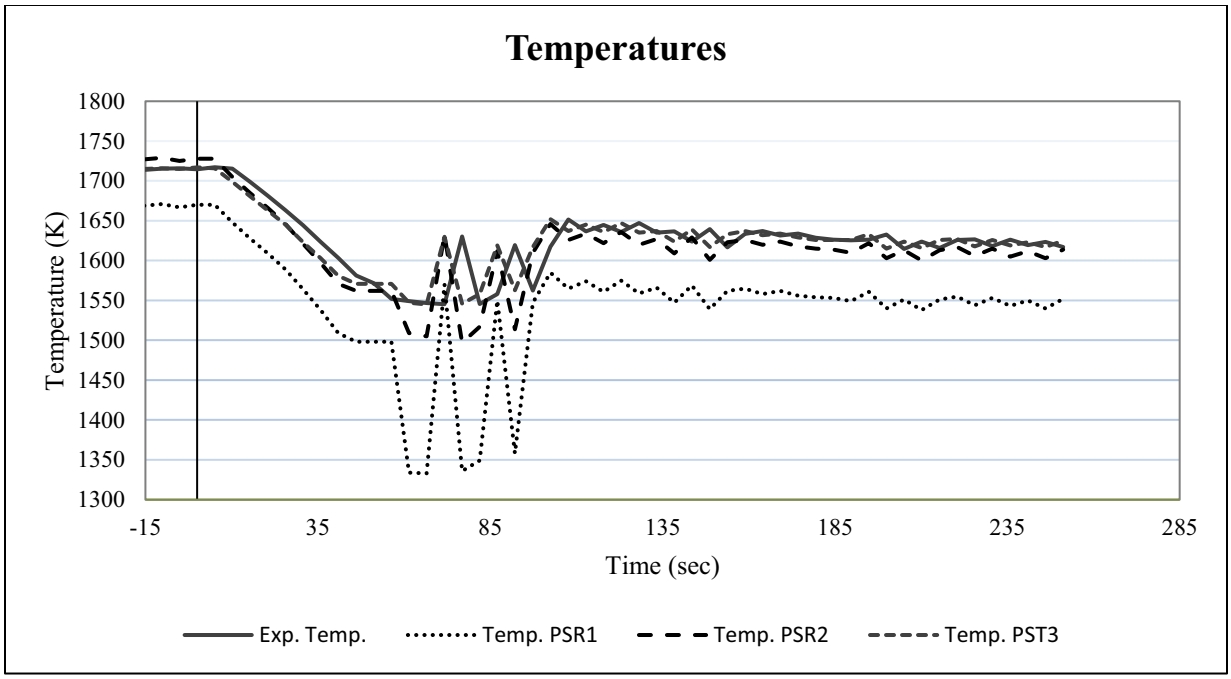

Figure A.24: Time variation of Temperatures (measured and computed) for Experiment set# 2, Case# 4

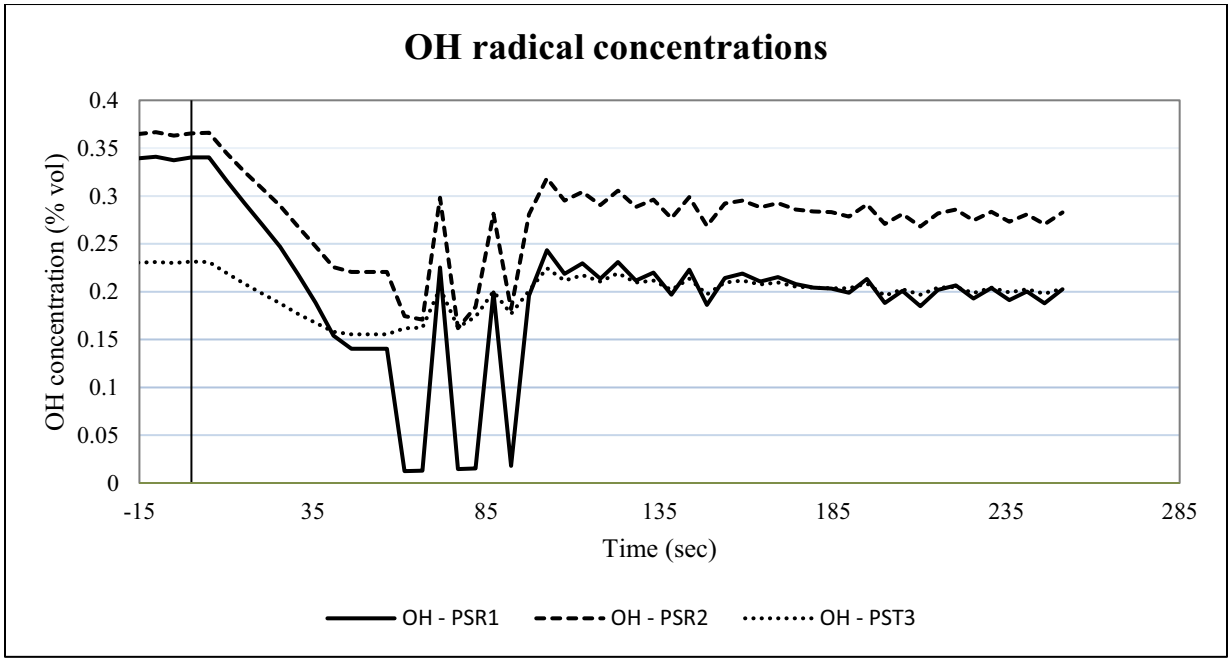

Figure A.25: Time variation of computed OH concentrations for Experiment set# 2, Case# 4

7. Experiment Set# 1, Case# 1: Gradual Air flow increase from 0.8 g/s to 1.2 g/s in 60 seconds

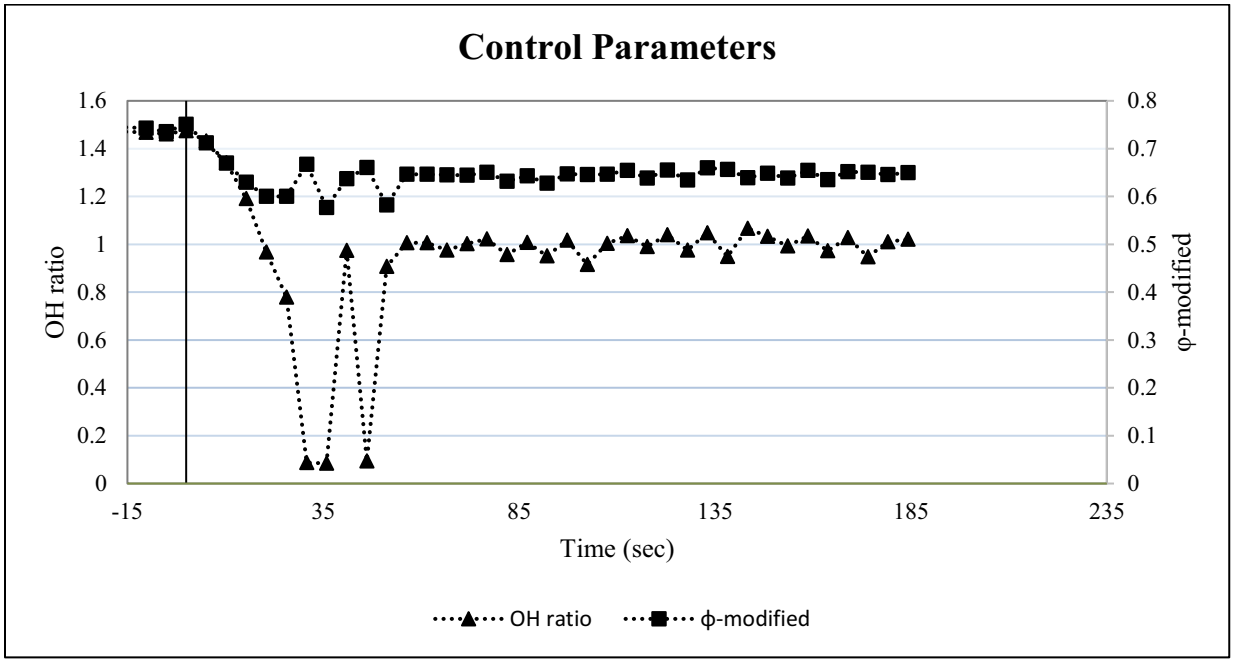

Figure A.26: Time variation of control parameters for Experiment set# 2, Case# 5

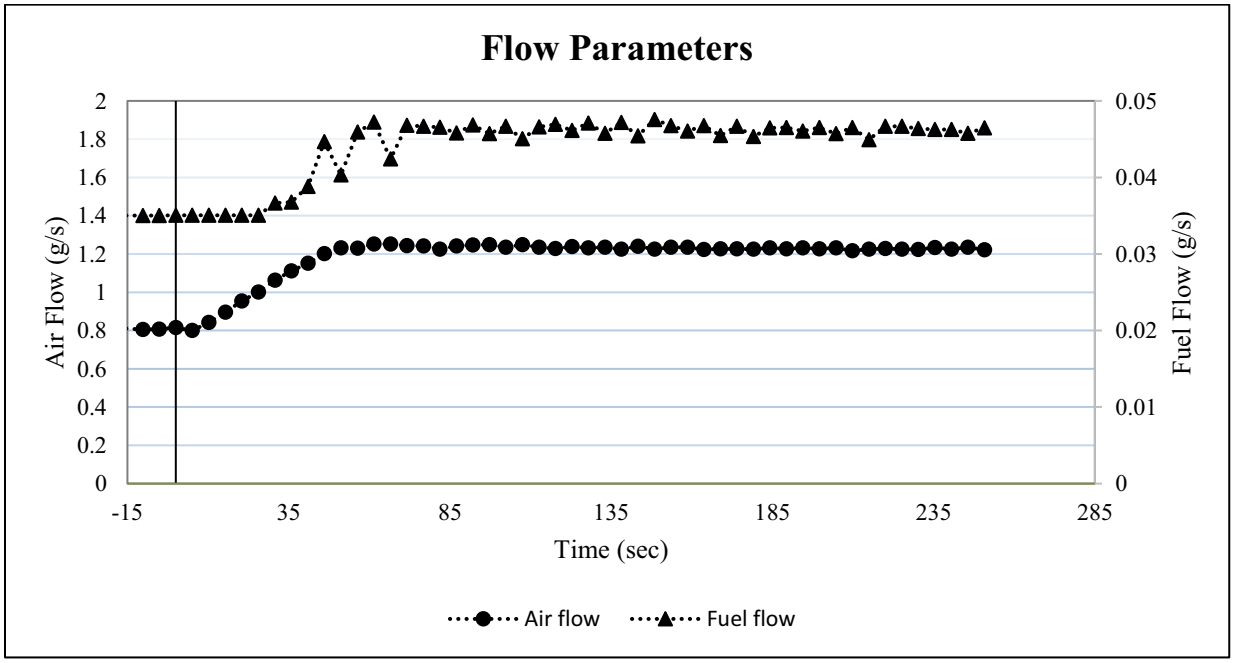

Figure A.27: Time variation of flow data for Experiment set# 2, Case# 5

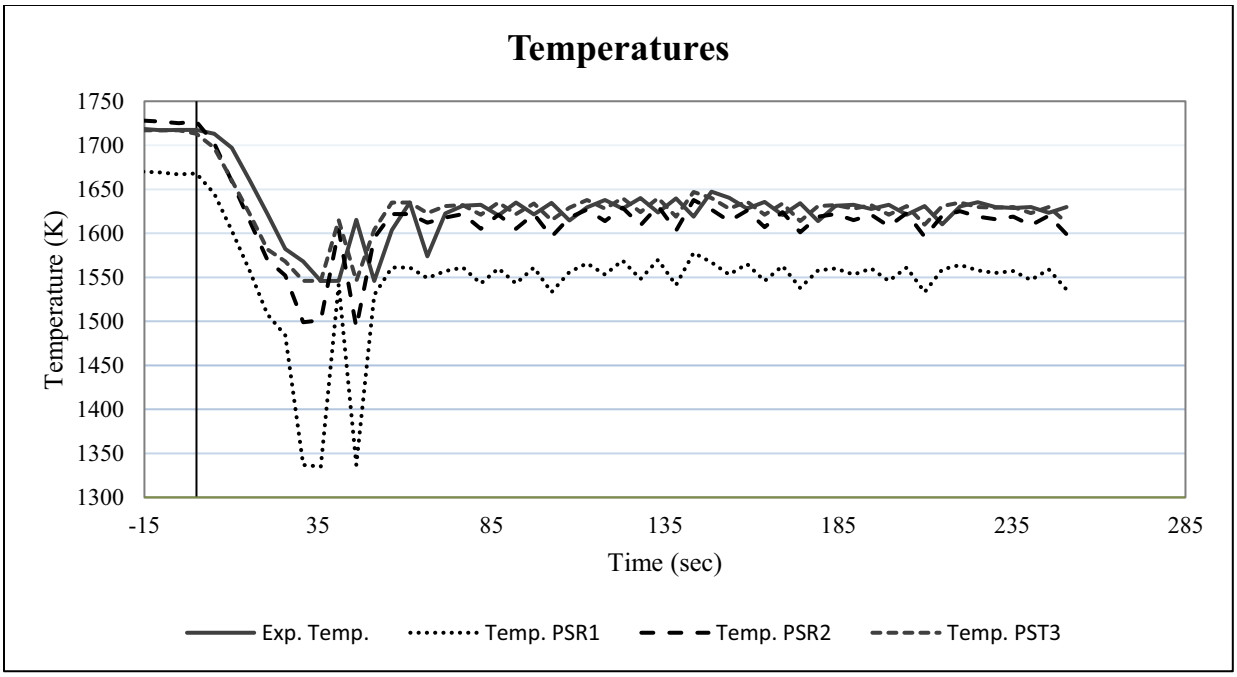

Figure A.28: Time variation of Temperatures (measured and computed) for Experiment set# 2, Case# 5

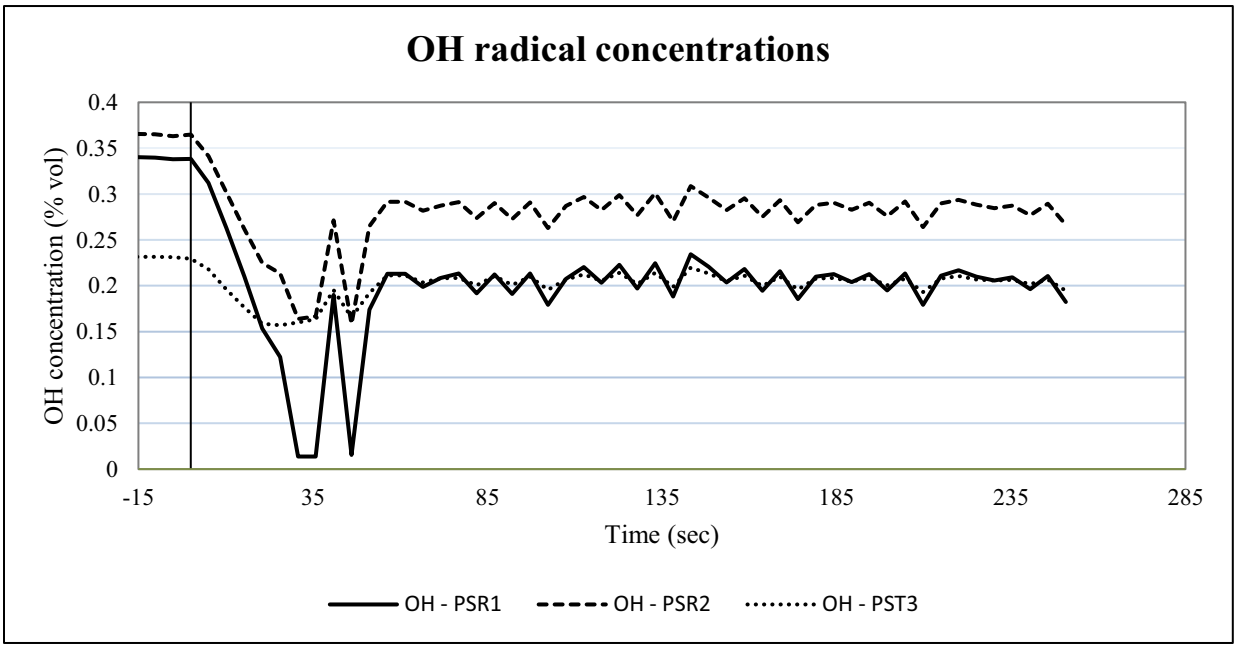

Figure A.29: Time variation of computed OH concentrations for Experiment set# 2, Case# 5

8. Experiment Set# 1, Case# 1: Gradual Air flow increase from 0.8 g/s to 1.2 g/s in 30 seconds

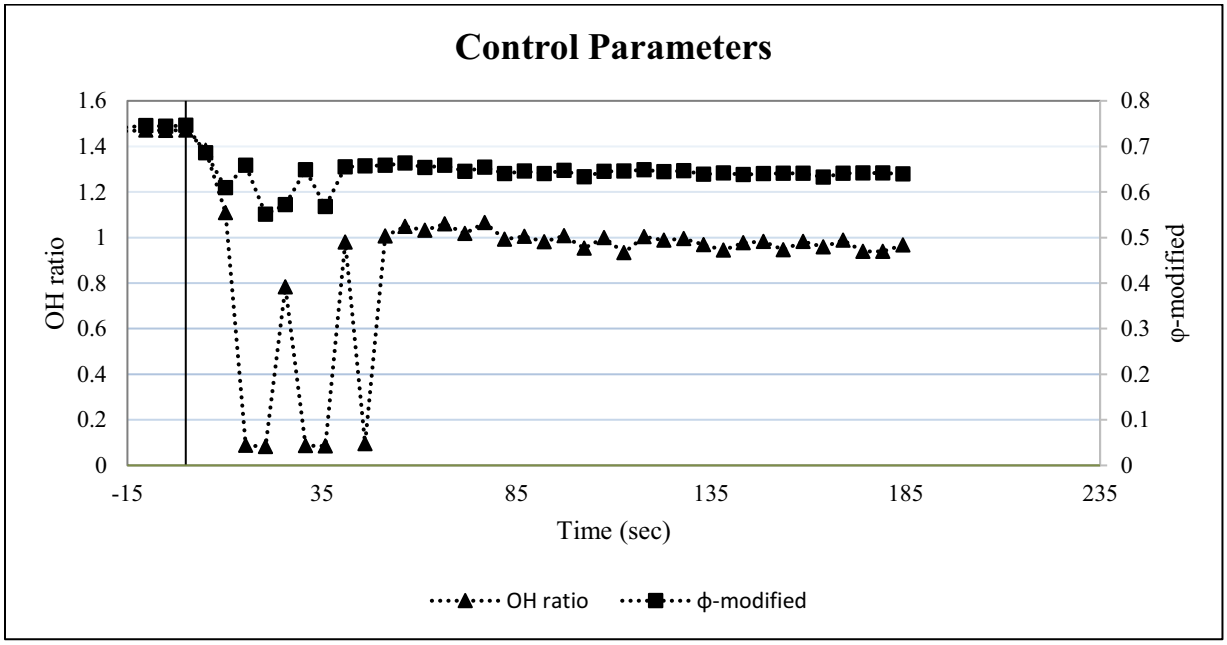

Figure A.30: Time variation of control parameters for Experiment set# 2, Case# 6

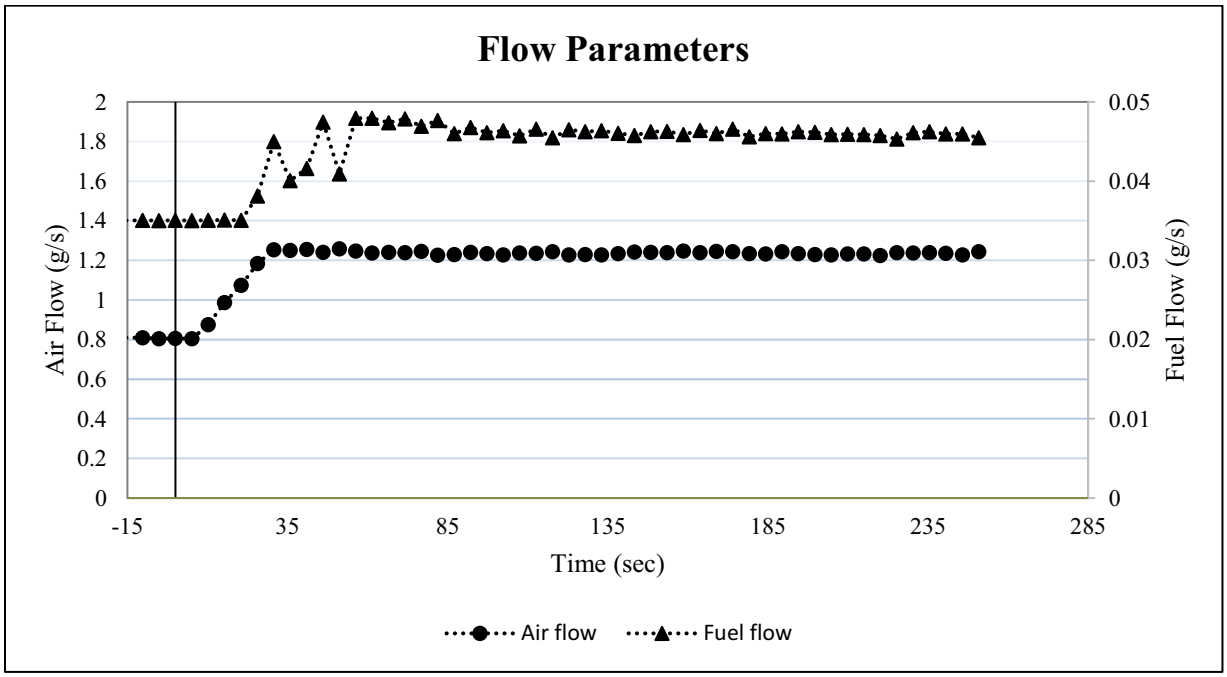

Figure A.31: Time variation of flow data for Experiment set# 2, Case# 6

+

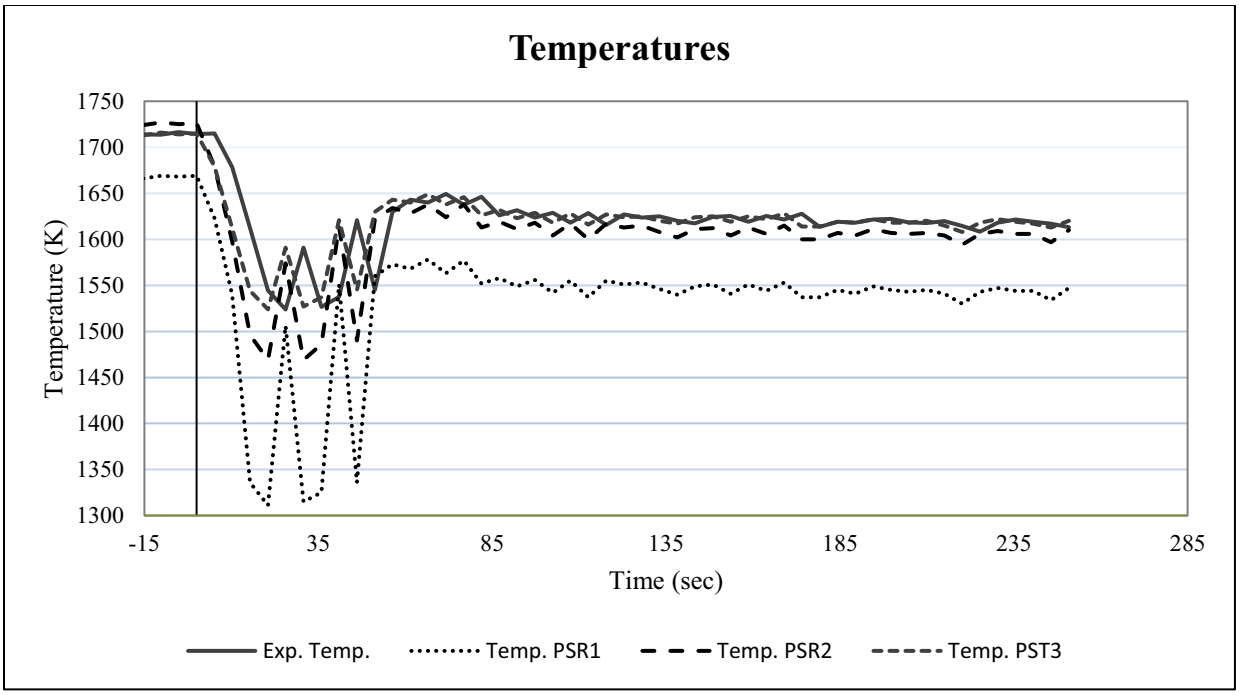

Figure A.32: Time variation of Temperatures (measured and computed) for Experiment set# 2, Case# 6

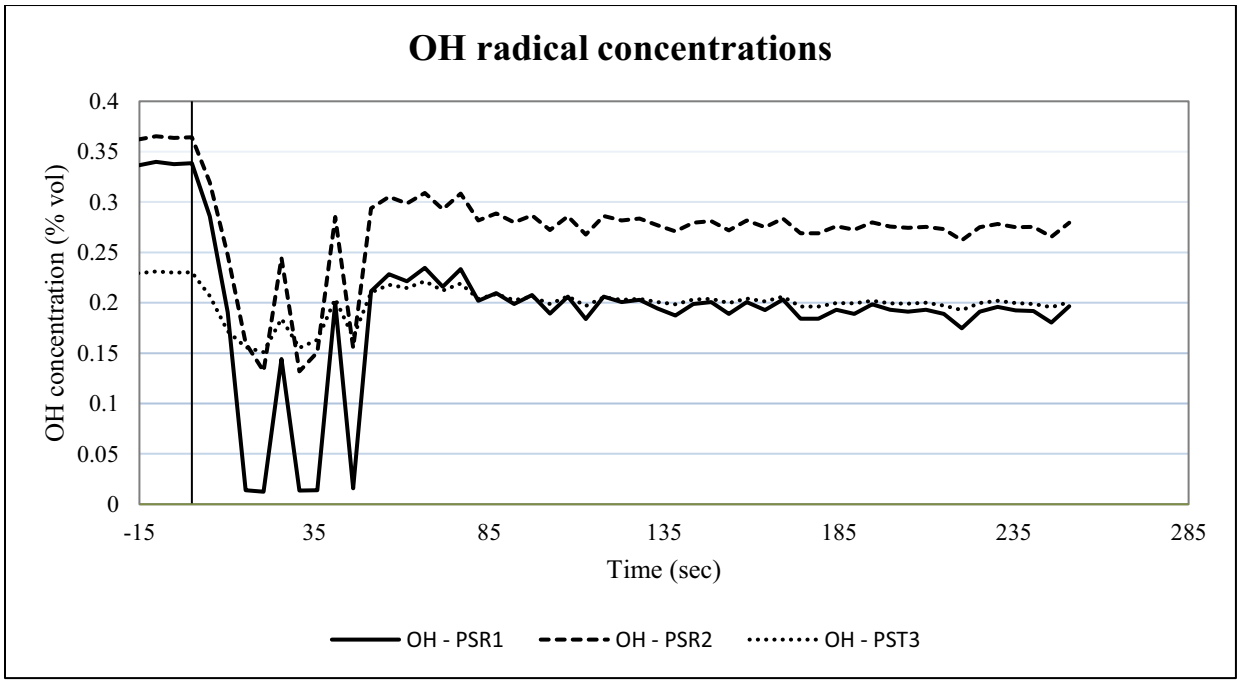

Figure A.33: Time variation of computed OH concentrations for Experiment set# 2, Case# 6

Appendix IV. CREK Code Modifications

The following piece of code has been added to the subroutine 'OUTPT' to add the LBO control functionality to the original CREK code:-

```
      OPEN(12,FILE='C:\Users\David\Desktop\CRN_CTRL\last.txt',STA
     +TUS='UNKNOWN')
      read (12,5400) ER_last,rOH_last
c     read (12,5500) rOH_last(1)
      close (12,status='keep')

      ER1=ER

      if (rOH.lt.0.5) then
        ER1=ER+0.1

      elseif ((rOH.lt.1.2).and.(rOH_last.lt.1.2)) then

          if (rOH.gt.1.05) then
                              ER1=ER_last+(0.25*(ER-ER_last)*(1.1-rOH_last)/(rOH-rOH_last))
          endif

          if (rOH.lt.0.95) then
                              ER1=ER_last+(0.25*(ER-ER_last)*(1-rOH_last)/(rOH-rOH_last))
          endif

          if ((rOH.ge.0.95).and.(rOH.le.1.05)) then
             ER1=ER
          endif

c          if (rOH.lt.0.2) then
c             ER1=ER +0.1
c          endif

      endif

      if (abs(ER-ER_last).le.0.001) ER1=ER
      if (abs(rOH-rOH_last).le.0.01) ER1=ER

           OPEN (12,FILE='C:\Users\David\Desktop\CRN_CTRL\last.txt',STATUS
     +='UNKNOWN')
      write(12,5400) ER,rOH
      close (12,status='keep')
```

This code makes the desired calculations for OH ratio and Φ-modified as per the algorithm and returns these values by appending them into the output text file from the CREK code. These values can be subsequently retrieved using LabVIEW and fed to the controllers.